J Nonlinear Sci (2016) 26:365–403
DOI 10.1007/s00332-015-9278-1

Journal of Nonlinear Science

Transverse Instability of Line Solitary Waves in Massive Dirac Equations

Dmitry Pelinovsky[1] · **Yusuke Shimabukuro**[1]

Received: 7 November 2014 / Accepted: 23 October 2015 / Published online: 6 November 2015

Abstract Working in the context of localized modes in periodic potentials, we consider two systems of the massive Dirac equations in two spatial dimensions. The first system, a generalized massive Thirring model, is derived for the periodic stripe potentials. The second one, a generalized massive Gross–Neveu equation, is derived for the hexagonal potentials. In both cases, we prove analytically that the line solitary waves are spectrally unstable with respect to periodic transverse perturbations of large periods. The spectral instability is induced by the spatial translation for the generalized massive Thirring model and by the gauge rotation for the generalized massive Gross–Neveu model. We also observe numerically that the spectral instability holds for the transverse perturbations of any period in the generalized massive Thirring model and exhibits a finite threshold on the period of the transverse perturbations in the generalized massive Gross–Neveu model.

Keywords Massive Thirring model · Massive Gross-Neveu equation · Line solitary waves · Transverse instability · Lyapunov-Schmidt reduction method · Chebyshev interpolation method

Mathematics Subject Classification 35Q41 · 37K40 · 37K45

Communicated by Michael I. Weinstein.

✉ Dmitry Pelinovsky
dmpeli@math.mcmaster.ca

[1] Department of Mathematics and Statistics, McMaster University, Hamilton, ON L8S 4K1, Canada

1 Introduction

Starting with pioneer contributions of V.E. Zakharov and his school (Zakharov and Rubenchik 1974), studies of transverse instabilities of line solitary waves in various nonlinear evolution equations have been developed in many different contexts. With the exception of the Kadomtsev–Petviashvili-II (KP-II) equation, line solitary waves in many evolution equations are spectrally unstable with respect to transverse periodic perturbations (Kivshar and Pelinovsky 2000).

More recently, it was proved for the prototypical model of the KP-I equation that the line solitary waves under the transverse perturbations of sufficiently small periods remain spectrally and orbitally stable (Rousset and Tzvetkov 2012). Similar thresholds on the period of transverse instability exist in other models such as the elliptic nonlinear Schrödinger (NLS) equation (Yamazaki 2015) and the Zakharov–Kuznetsov (ZK) equation (Pelinovsky et al. 2015). Nevertheless, this conclusion is not universal and the line solitary waves can be spectrally unstable for all periods of the transverse perturbations, as it happens for the hyperbolic NLS equation (Pelinovsky et al. 2014).

Conclusions on the transverse stability or instability of line solitary waves may change in the presence of the periodic potentials. In the two-dimensional problems with square periodic potentials, it was found numerically in Hoq et al. (2009), Kevrekidis et al. (2007), Yang (2011) that line solitary waves are spectrally stable with respect to periodic transverse perturbations if they bifurcate from the so-called X point of the Brillouin zone. Line solitary waves remain spectrally unstable if they bifurcate from the Γ point of the Brillouin zone. These numerical results are rigorously justified in Pelinovsky and Yang (2014) from the analysis of the two-dimensional discrete NLS equation, which models the tight-binding limit of the periodic potentials (Pelinovsky and Schneider 2010).

For the one-dimensional periodic (stripe) potentials, similar stabilization of the line solitary waves was observed numerically in Yang et al. (2012). In the contrast to these results, it was proven within the tight-binding limit in Pelinovsky and Yang (2014) that transverse instabilities of line solitary waves persist for any parameter configurations of the discrete NLS equation. One of the motivations for our present work is to inspect whether the line solitary waves become spectrally stable with respect to the periodic transverse perturbations in periodic stripe potentials far away from the tight-binding limit.

In particular, we employ the massive Dirac equations also known as the coupled-mode equations, which have been derived and justified in the reduction of the Gross–Pitaevskii equation with small periodic potentials (Schneider and Uecker 2001). Similar models were also introduced in the context of the periodic stripe potentials in Dohnal and Aceves (2005), where the primary focus was on the existence and stability of fully localized two-dimensional solitary waves. From the class of massive Dirac models, we will be particularly interested in a generalization of the massive Thirring model (Thirring 1958), for which orbital stability of one-dimensional solitons was proved in our previous work with the help of conserved quantities (Pelinovsky and Shimabukuro 2014) and auto-Bäcklund transformation (Contreras et al. 2013). In the present work, we prove analytically that the line solitary waves of the massive Thirring model in two spatial dimensions are spectrally unstable with respect to the periodic transverse perturbations of large periods. The spectral instability is induced by the spatial translation of the line solitary waves. We also show numerically that the instability persists for smaller periods of transverse perturbations.

In the context of numerical results in Yang et al. (2012), we now confirm that line solitary waves in the periodic stripe potential remain spectrally unstable with respect to periodic transverse perturbations both in the tight-binding and small-potential limits. The numerical results in Yang et al. (2012) are observed apparently in a narrow interval of the existence domain for the line solitary waves supported by the periodic stripe potential.

Different versions of the massive Dirac equations were derived recently in the context of hexagonal potentials. The corresponding systems generalize the massive Gross–Neveu model [also known as the Soler model in $(1+1)$ dimensions] (Gross and Neveu 1974). These equations are derived formally in Ablowitz and Zhu (2012, 2013) and are justified recently in Fefferman and Weinstein (2012a, 2014). Extending the scope of our work, we prove analytically that the line solitary waves of the massive Gross–Neveu model in two spatial dimensions are also spectrally unstable with respect to the periodic perturbations of large periods. The spectral instability is induced by the gauge rotation. Numerical results indicate that the instability exhibits a finite threshold on the period of the transverse perturbations.

The method we employ in our work is relatively old (Zakharov and Rubenchik 1974) [see review in Kivshar and Pelinovsky (2000)], although it has not been applied to the class of massive Dirac equations even at the formal level. We develop analysis at the rigorous level of arguments. Our work relies on the resolvent estimates for the spectral stability problem in $(1+1)$ dimensions, where the zero eigenvalue is disjoint from the continuous spectrum, whereas the eigenfunctions for the zero eigenvalue are known from the translational and gauge symmetries of the massive Dirac equations. When the transverse wave number is nonzero but small, the multiple zero eigenvalue splits and one can rigorously justify whether this splitting induces the spectral instability or not. It becomes notoriously more difficult to prove persistence of instabilities for large transverse wave numbers (small periods); hence, we have to retreat to numerical computations for such studies of the corresponding transverse stability problem.

The approach we undertake in this paper is complementary to the computations based on the Evans function method (Johnson 2010; Johnson and Zumbrun 2010). Although both approaches stand on rigorous theory based on the implicit function theorem, we believe that the perturbative computations are shorter and provide the binary answer on the spectral stability or instability of the line solitary wave with respect to periodic transverse perturbations in a simple and concise way.

The structure of this paper is as follows. Section 2 introduces two systems of the massive Dirac equations and their line solitary waves in the context of stripe and hexagonal potentials. Section 3 presents the analytical results and gives details of algorithmic computations of the perturbation theory for the massive Thirring and Gross–Neveu models in two spatial dimensions. Section 4 contains numerical approximations of eigenvalues of the spectral stability problem. Transverse instabilities of small-amplitude line solitary waves in more general massive Dirac models are discussed in Sect. 5.

2 Massive Dirac Equations

The class of massive Dirac equations on the line can be written in the following general form (Chugunova and Pelinovsky 2006; Pelinovsky 2011),

$$\begin{cases} i(u_t + u_x) + v = \partial_{\bar{u}} W(u, v, \bar{u}, \bar{v}), \\ i(v_t - v_x) + u = \partial_{\bar{v}} W(u, v, \bar{u}, \bar{v}), \end{cases} \quad x \in \mathbb{R}, \tag{2.1}$$

where the subscripts denote partial differentiation, (u, v) are complex-valued amplitudes in spatial x and temporal t variables, and W is the real function of $(u, v, \bar{u}, \bar{v})$, which is symmetric with respect to u and v and satisfies the gauge invariance

$$W(\mathrm{e}^{i\alpha}u, \mathrm{e}^{i\alpha}v, \mathrm{e}^{-i\alpha}\bar{u}, \mathrm{e}^{-i\alpha}\bar{v}) = W(u, v, \bar{u}, \bar{v}) \quad \text{for every} \quad \alpha \in \mathbb{R}.$$

As it is shown in Chugunova and Pelinovsky (2006), under the constraints on W, it can be expressed in terms of variables $(|u|^2 + |v|^2)$, $|u|^2|v|^2$, and $(\bar{u}v + u\bar{u})$. For the cubic Dirac equations, W is a homogeneous quartic polynomial in u and v, which is written in the most general form as

$$W = c_1(|u|^2 + |v|^2)^2 + c_2|u|^2|v|^2 + c_3(|u|^2 + |v|^2)(\bar{u}v + u\bar{v}) + c_4(\bar{u}v + u\bar{v})^2,$$

where c_1, c_2, c_3, and c_4 are real coefficients. In this case, a family of stationary solitary waves of the massive Dirac equations can be found in the explicit form (Chugunova and Pelinovsky 2006) [see also Mertens et al. (2012)].

Among various nonlinear Dirac equations, the following particular cases have profound significance in relativity theory:

- $W = |u|^2|v|^2$—the massive Thirring model (Thirring 1958);
- $W = \frac{1}{2}(\bar{u}v + u\bar{v})^2$—the massive Gross–Neveu model (Gross and Neveu 1974).

Global well-posedness of the massive Thirring model was proved both in $H^s(\mathbb{R})$ for $s > \frac{1}{2}$ (Selberg and Tesfahun 2010) and in $L^2(\mathbb{R})$ (Candy 2011). Recently, global well-posedness of the massive Gross–Neveu equations was proved both in $H^s(\mathbb{R})$ for $s > \frac{1}{2}$ (Huh 2013) and in $L^2(\mathbb{R})$ (Zhang and Zhao 2015).

When the massive Dirac equations are used in modeling of the Gross–Pitaevskii equation with small periodic potentials, the realistic nonlinear terms are typically different from the two particular cases of the massive Thirring and Gross–Neveu models. (In this context, the nonlinear Dirac equations are also known as the coupled-mode equations.) In the following two subsections, we describe the connection of the generalized massive Thirring and Gross–Neveu models in two spatial dimensions to physics of nonlinear states of the Gross–Pitaevskii equation trapped in periodic potentials.

2.1 Periodic Stripe Potentials

In the context of one-dimensional periodic (stripe) potentials, the massive Dirac equations (2.1) can be derived in the following form (Dohnal and Aceves 2005),

$$\begin{cases} i(u_t + u_x) + v + u_{yy} = (\alpha_1|u|^2 + \alpha_2|v|^2)u, \\ i(v_t - v_x) + u + v_{yy} = (\alpha_2|u|^2 + \alpha_1|v|^2)v, \end{cases} \quad (x, y) \in \mathbb{R}^2, \tag{2.2}$$

where y is a new coordinate in the transverse direction to the stripe potential, the complex-valued amplitudes (u, v) correspond to two counter-propagating resonant Fourier modes interacting with the small periodic potential, and (α_1, α_2) are real-valued parameters. For the stripe potentials, the parameters satisfy the constraint $\alpha_2 = 2\alpha_1$.

To illustrate the derivation of the massive Dirac equations (2.2), we can consider a two-dimensional Gross–Pitaevskii equation with a small periodic potential

$$i\psi_t = -\psi_{xx} - \psi_{yy} + 2\epsilon\cos(x)\psi + |\psi|^2\psi, \tag{2.3}$$

and apply the Fourier decomposition

$$\psi(x, y, t) = \sqrt{\epsilon}\left[u(\epsilon x, \sqrt{\epsilon}y, \epsilon t)\mathrm{e}^{\frac{i}{2}x - \frac{i}{4}t} + v(\epsilon x, \sqrt{\epsilon}y, \epsilon t)\mathrm{e}^{-\frac{i}{2}x - \frac{i}{4}t} + \epsilon R(x, y, t)\right], \tag{2.4}$$

where ϵ is a small parameter and R is the remainder term. From the condition that R is bounded in variables (x, y, t), it can be obtained from (2.3) and (2.4) that (u, v) satisfy the nonlinear Dirac equations (2.2) with $\alpha_1 = 1$ and $\alpha_2 = 2$. Justification of the Fourier decomposition (2.4) and the nonlinear Dirac equations (2.2) in the context of the Gross–Pitaevskii equation (2.3) has been reported for y-independent perturbations in Schneider and Uecker (2001). Transverse modulations can be taken into account in the same justification procedure, since the error R is bounded in the supremum norm, whereas the solution of the massive Dirac equations (2.2) and the solution of the Gross–Pitaevskii equation (2.3) can be defined in Sobolev spaces of sufficiently high regularity [see Chapter 2.2 in Pelinovsky (2011)].

The stationary y-independent solitary waves of the massive Dirac equations (2.2) are referred to as the line solitary waves. According to the analysis in Chugunova and Pelinovsky (2006), Mertens et al. (2012), the corresponding solutions can be represented in the form

$$u(x, t) = U_\omega(x)\mathrm{e}^{i\omega t}, \quad v(x, t) = \bar{U}_\omega(x)\mathrm{e}^{i\omega t}, \tag{2.5}$$

where $\omega \in (-1, 1)$ is taken in the gap between two branches of the linear wave spectrum of the massive Dirac equations (2.2). The complex-valued amplitude U_ω satisfies the first-order differential equation

$$iU'_\omega - \omega U_\omega + \overline{U}_\omega = (\alpha_1 + \alpha_2)|U_\omega|^2 U_\omega. \tag{2.6}$$

In terms of physical applications, the line solitary wave (2.5) of the massive Dirac equations (2.2) corresponds to a localized mode (the so-called gap soliton) trapped by the periodic stripe potential (Pelinovsky 2011).

In our work, we perform transverse spectral stability analysis of the line solitary waves (2.5) for the particular configuration $\alpha_1 = 0$ and $\alpha_2 = 1$, which correspond to the massive Thirring model on the line (Thirring 1958). If $\alpha_1 = 0$ and $\alpha_2 = 1$, the solitary wave solution of the differential equation (2.6) exists for every $\omega \in (-1, 1)$ in the explicit form

$$U_\omega(x) = \sqrt{2}\mu \frac{\sqrt{1+\omega}\cosh(\mu x) - i\sqrt{1-\omega}\sinh(\mu x)}{\omega + \cosh(2\mu x)}, \tag{2.7}$$

where $\mu = \sqrt{1-\omega^2}$. The solitary wave solution of the differential equation (2.6) is unique up to the translational and gauge transformation. As $\omega \to 1$, the family of solitary waves (2.7) approaches the NLS profile $U_{\omega\to 1}(x) \to \mu \text{sech}(\mu x)$. As $\omega \to -1$, it degenerates into the algebraic profile

$$U_{\omega=-1}(x) = \frac{2(1-2ix)}{1+4x^2}.$$

When y-independent perturbations are considered, solitary waves (2.5) and (2.7) are orbitally stable in the time evolution of the massive Thirring model on the line for every $\omega \in (-1, 1)$. The corresponding results were obtained in our previous works (Pelinovsky and Shimabukuro 2014) in $H^1(\mathbb{R})$ and (Contreras et al. 2013) in a weighted subspace of $L^2(\mathbb{R})$. Note that the solitary waves in more general nonlinear Dirac equations (2.2) are spectrally unstable for y-independent perturbations if $\alpha_1 \neq 0$, but the instability region and the number of unstable eigenvalues depend on the parameter ω (Chugunova and Pelinovsky 2006).

We will show (see Theorem 3.3 below) that the line solitary waves (2.5) and (2.7) for $\alpha_1 = 0$ and $\alpha_2 = 1$ are spectrally unstable with respect to long periodic transverse perturbations for every $\omega \in (-1, 1)$. In the more general massive Dirac equations (2.2), we also show (see Sect. 5.1 below) that the instability conclusion remains true at least in the small-amplitude limit (when either $\omega \to 1$ or $\omega \to -1$) if $\alpha_1 + \alpha_2 \neq 0$.

2.2 Hexagonal Potentials

In the context of the hexagonal potentials in two spatial dimensions, the massive Dirac equations can be derived in a different form (Fefferman and Weinstein 2012b),

$$\begin{cases} i\partial_t\varphi_1 + i\partial_x\varphi_2 - \partial_y\varphi_2 + \varphi_1 = (\beta_1|\varphi_1|^2 + \beta_2|\varphi_2|^2)\varphi_1, \\ i\partial_t\varphi_2 + i\partial_x\varphi_1 + \partial_y\varphi_1 - \varphi_2 = (\beta_2|\varphi_1|^2 + \beta_1|\varphi_2|^2)\varphi_2, \end{cases} \quad (x, y) \in \mathbb{R}^2, \tag{2.8}$$

where (φ_1, φ_2) are complex-valued amplitudes for two resonant Floquet–Bloch modes in the hexagonal lattice and (β_1, β_2) are real-valued positive parameters. The nonlinear Dirac equations (2.8) correspond to equations (4.4)–(4.5) in Fefferman and Weinstein

(2012b). Derivation of these equations can also be found in Ablowitz and Zhu (2012, 2013). Justification of the linear part of these equations is performed by Fefferman and Weinstein (2014).

To transform the nonlinear Dirac equations (2.8) to the form (2.1), we use the change of variables,

$$\begin{pmatrix} u \\ v \end{pmatrix} = \frac{1}{2}\begin{pmatrix} 1 & 1 \\ 1 & -1 \end{pmatrix}\begin{pmatrix} \varphi_1 \\ \varphi_2 \end{pmatrix},$$

and obtain

$$\begin{cases} i(u_t + u_x) + v + v_y = \beta_1(u|u|^2 + \overline{u}v^2 + 2u|v|^2) + \beta_2\overline{u}(u^2 - v^2), \\ i(v_t - v_x) + u - u_y = \beta_1(v|v|^2 + \overline{v}u^2 + 2v|u|^2) + \beta_2\overline{v}(v^2 - u^2). \end{cases} \tag{2.9}$$

In comparison with the nonlinear Dirac equations (2.2), we note that both the cubic nonlinearities and the y-derivative diffractive terms are different.

For the family of line solitary waves (2.5), the complex-valued amplitude U_ω satisfies the first-order differential equation

$$iU_\omega' - \omega U_\omega + \overline{U}_\omega = (3\beta_1 + \beta_2)U_\omega|U_\omega|^2 + (\beta_1 - \beta_2)\overline{U}_\omega^3. \tag{2.10}$$

In terms of physical applications, the line solitary wave (2.5) of the massive Dirac equations (2.9) corresponds to a localized mode trapped by the deformed hexagonal potential with broken Dirac points (Ablowitz and Zhu 2013; Fefferman and Weinstein 2012b).

In what follows, we perform the transverse spectral stability analysis of the line solitary waves (2.5) for the particular configuration $\beta_1 = -\beta_2 = \frac{1}{2}$, which corresponds to the massive Gross–Neveu model on the line (Gross and Neveu 1974). If $\beta_1 = -\beta_2 = \frac{1}{2}$, the solitary wave solution of the differential equation (2.10) exists for every $\omega \in (0, 1)$ in the explicit form

$$U_\omega(x) = \mu\frac{\sqrt{1+\omega}\cosh(\mu x) - i\sqrt{1-\omega}\sinh(\mu x)}{1 + \omega\cosh(2\mu x)}, \tag{2.11}$$

where $\mu = \sqrt{1-\omega^2}$. Again the solitary wave solution of the differential equation (2.10) is unique up to the translational and gauge transformation. The family of solitary waves (2.11) diverges at infinity as $\omega \to 0$ and cannot be continued for $\omega \in (-1, 0)$ (Berkolaiko et al. 2015). As $\omega \to 1$, the family approaches the NLS profile $U_{\omega\to 1}(x) \to 2^{-1/2}\mu\text{sech}(\mu x)$.

When y-independent perturbations are considered, solitary waves (2.5) and (2.11) are orbitally stable in $H^1(\mathbb{R})$ in the time evolution of the massive Gross–Neveu model for $\omega \approx 1$ (Boussaid and Comech 2012). Regarding spectral stability, two numerical studies exist, which show contradictory results to each other. A numerical approach based on the Evans function computation leads to the conclusion on the spectral stability of solitary waves for all $\omega \in (0, 1)$ (Berkolaiko et al. 2015; Berkolaiko and Comech 2012). However, another approach based on the finite difference discretization indicates existence of $\omega_c \approx 0.6$ such that the family of solitary waves is spectrally stable for $\omega \in (\omega_c, 1)$ and unstable for $\omega \in (0, \omega_c)$ (Mertens et al. 2012; Shao et al. 2014). The presence of additional unstable eigenvalues in the case of y-independent perturbations, if they exist, is not an obstacle in our analysis of transverse stability of line solitary waves.

Our work concerns both y-independent and y-dependent perturbations. In the case of y-independent perturbations, we show numerically (see Sect. 4.2 below) that the solitary waves of the massive Gross–Neveu model are spectrally stable for every $\omega \in (0, 1)$, thus supporting the numerical results of Berkolaiko et al. (2015), Berkolaiko and Comech (2012) with an independent numerical method based on the Chebyshev interpolation method. In the case of y-periodic perturbations, we show analytically (see Theorem 3.3 below) that the line solitary waves (2.5) and (2.11) for $\beta_1 = -\beta_2 = \frac{1}{2}$ are spectrally unstable with respect to long periodic transverse perturbations for every $\omega \in (0, 1)$. In the more general massive Dirac equations (2.9), we also show (see Sect. 5.2 below) that the instability conclusion remains true at least in the small-amplitude limit (when either $\omega \to 1$ or $\omega \to -1$) if $\beta_1 \neq 0$.

3 Transverse Spectral Stability of Line Solitary Waves

We consider two versions (2.2) and (2.9) of the nonlinear Dirac equations for spatial variables (x, y) in the domain $\mathbb{R} \times \mathbb{T}$, where $\mathbb{T} = \mathbb{R}/(L\mathbb{Z})$ is the one-dimensional torus and $L \in \mathbb{R}$ is the period of the transverse perturbation. To study stability of the line solitary wave (2.5) under periodic transverse perturbations, we use the Fourier series and write

$$u(x, y, t) = \mathrm{e}^{i\omega t} \left[U_\omega(x) + \sum_{n \in \mathbb{Z}} \hat{f}_n(x, t) \mathrm{e}^{\frac{2\pi n i y}{L}} \right]. \tag{3.1}$$

In the setting of the spectral stability theory, we are going to use the linear superposition principle and consider just one Fourier mode with continuous parameter $p \in \mathbb{R}$. In the context of the Fourier series (3.1), the parameter p takes the countable set of values $\{\frac{2\pi n}{L}\}_{n \in \mathbb{Z}}$. The limit $p \to 0$ corresponds to the limit of long periodic perturbations with $L \to \infty$.

For each $p \in \mathbb{R}$, we separate the time evolution of the linearized system and introduce the spectral parameter λ in the decomposition $\hat{f}_n(x, t) = \hat{F}_n(x)\mathrm{e}^{\lambda t}$. This decomposition reduces the linearized equations for $\hat{f}_n$ to the eigenvalue problem for $\hat{F}_n$ and λ. Performing similar manipulations with four components of the nonlinear Dirac equations, we set the transverse perturbation in the form

$$\begin{aligned} u(x, y, t) &= \mathrm{e}^{i\omega t}[U_\omega(x) + u_1(x)\mathrm{e}^{\lambda t + ipy}], & \bar{u}(x, y, t) &= \mathrm{e}^{-i\omega t}[\overline{U}_\omega(x) + u_2(x)\mathrm{e}^{\lambda t + ipy}], \\ v(x, y, t) &= \mathrm{e}^{i\omega t}[\overline{U}_\omega(x) + v_1(x)\mathrm{e}^{\lambda t + ipy}], & \bar{v}(x, y, t) &= \mathrm{e}^{-i\omega t}[U_\omega(x) + v_2(x)\mathrm{e}^{\lambda t + ipy}]. \end{aligned}$$

Remark 1 Since the perturbation to the line solitary wave is just one linear mode, the component (u_2, v_2) is not the complex conjugate of (u_1, v_1). However, given a solution (u_1, u_2, v_1, v_2) of the eigenvalue problem for λ and p, there exists another solution $(\bar{u}_2, \bar{u}_1, \bar{v}_2, \bar{v}_1)$ of the same eigenvalue problem for $\bar{\lambda}$ and $-p$.

Let $\mathbf{F} = (u_1, u_2, v_1, v_2)^t$. The eigenvalue problem for $\mathbf{F}$ and λ can be written in the form

$$i\lambda\sigma\mathbf{F} = (D_\omega + E_p + W_\omega)\mathbf{F}, \tag{3.2}$$

where

$$D_\omega = \begin{bmatrix} -i\partial_x + \omega & 0 & -1 & 0 \\ 0 & i\partial_x + \omega & 0 & -1 \\ -1 & 0 & i\partial_x + \omega & 0 \\ 0 & -1 & 0 & -i\partial_x + \omega \end{bmatrix}, \quad \sigma = \begin{bmatrix} 1 & 0 & 0 & 0 \\ 0 & -1 & 0 & 0 \\ 0 & 0 & 1 & 0 \\ 0 & 0 & 0 & -1 \end{bmatrix},$$

whereas matrices E_p and W_ω depend on the particular form of the nonlinear Dirac equations. For the model (2.2) with $\alpha_1 = 0$ and $\alpha_2 = 1$, we obtain $E_p = p^2 I$ with

$$I = \begin{bmatrix} 1 & 0 & 0 & 0 \\ 0 & 1 & 0 & 0 \\ 0 & 0 & 1 & 0 \\ 0 & 0 & 0 & 1 \end{bmatrix} \quad \text{and} \quad W_\omega = \begin{bmatrix} |U_\omega|^2 & 0 & U_\omega^2 & |U_\omega|^2 \\ 0 & |U_\omega|^2 & |U_\omega|^2 & \overline{U}_\omega^2 \\ \overline{U}_\omega^2 & |U_\omega|^2 & |U_\omega|^2 & 0 \\ |U_\omega|^2 & U_\omega^2 & 0 & |U_\omega|^2 \end{bmatrix}, \tag{3.3}$$

where U_ω is given by (2.7). For the model (2.9) with $\beta_1 = -\beta_2 = \frac{1}{2}$, we obtain $E_p = -ipJ$ with

$$J = \begin{bmatrix} 0 & 0 & 1 & 0 \\ 0 & 0 & 0 & 1 \\ -1 & 0 & 0 & 0 \\ 0 & -1 & 0 & 0 \end{bmatrix} \quad \text{and}$$

$$W_\omega = \begin{bmatrix} |U_\omega|^2 & \bar{U}_\omega^2 & U_\omega^2 + 2\overline{U}_\omega^2 & |U_\omega|^2 \\ U_\omega^2 & |U_\omega|^2 & |U_\omega|^2 & 2U_\omega^2 + \overline{U}_\omega^2 \\ 2U_\omega^2 + \overline{U}_\omega^2 & |U_\omega|^2 & |U_\omega|^2 & U_\omega^2 \\ |U_\omega|^2 & U_\omega^2 + 2\overline{U}_\omega^2 & \overline{U}_\omega^2 & |U_\omega|^2 \end{bmatrix}, \tag{3.4}$$

where U_ω is now given by (2.11).

Remark 2 Let us denote the existence interval for the line solitary wave (2.5) of the nonlinear Dirac equations (2.1) by $\Omega \subset (-1, 1)$. For the model (2.2) with $\alpha_1 = 0$ and $\alpha_2 = 1$, we have $\Omega = (-1, 1)$. For the model (2.9) with $\beta_1 = -\beta_2 = \frac{1}{2}$, we have $\Omega = (0, 1)$.

The linear operator $D_\omega + E_p + W_\omega$ is self-adjoint in $L^2(\mathbb{R}, \mathbb{C}^4)$ with the domain in $H^1(\mathbb{R}, \mathbb{C}^4)$ thanks to the boundness of the potential term W_ω. We shall use the notation $\langle \cdot, \cdot \rangle_{L^2}$ for the inner product in $L^2(\mathbb{R}, \mathbb{C}^4)$ and the notation $\| \cdot \|_{L^2}$ for the induced norm. Our convention is to apply complex conjugation to the element at the first position of the inner product $\langle \cdot, \cdot \rangle_{L^2}$.

The next elementary result shows that the zero eigenvalue is isolated from the continuous spectrum of the spectral stability problem (3.2) both for $E_p = p^2 I$ and $E_p = -ipJ$ if the real parameter p is sufficiently small.

Proposition 3.1 *Assume that $W_\omega(x) \to 0$ as $|x| \to \infty$ according to an exponential rate. For every $\omega \in \Omega$ and every $p \in \mathbb{R}$, the continuous spectrum of the stability problem* (3.2) *is located along the segments $\pm i\Lambda_1$ and $\pm i\Lambda_2$, where for $E_p = p^2 I$,*

$$\Lambda_1 := \left\{ \sqrt{1+k^2} + \omega + p^2, \quad k \in \mathbb{R} \right\}, \quad \Lambda_2 := \left\{ \sqrt{1+k^2} - \omega - p^2, \quad k \in \mathbb{R} \right\}, \tag{3.5}$$

whereas for $E_p = -ipJ$,

$$\Lambda_1 := \left\{ \sqrt{1+p^2+k^2} + \omega, \quad k \in \mathbb{R} \right\}, \quad \Lambda_2 := \left\{ \sqrt{1+p^2+k^2} - \omega, \quad k \in \mathbb{R} \right\}. \tag{3.6}$$

Proof By Weyl's lemma, the continuous spectrum of the stability problem (3.2) coincides with the purely continuous spectrum of the same problem with $W_\omega \equiv 0$, thanks to the exponential decay of the potential terms W_ω to zero as $|x| \to \infty$. If $W_\omega \equiv 0$, we solve the spectral stability problem (3.2) with the Fourier transform in x, which means that we simply replace ∂_x in the operator D_ω with ik for $k \in \mathbb{R}$ and denote the resulting matrix by $D_{\omega,k}$. As a result, we obtain the matrix eigenvalue problem

$$(D_{\omega,k} + E_p - i\lambda\sigma)\mathbf{F} = 0.$$

After elementary algebraic manipulations, the characteristic equation for this linear system yields four solutions for λ given by $\pm i\Lambda_1$ and $\pm i\Lambda_2$, where the explicit expressions for Λ_1 and Λ_2 are given by (3.5) and (3.6) for $E_p = p^2 I$ and $E_p = -ipJ$, respectively. □

Remark 3 We note the different role of the matrix E_p in the location of the continuous spectrum for larger values of the real parameter p. If $E_p = p^2 I$, then the two bands $\pm i\Lambda_2$ touch each other for $|p| = p_\omega := \sqrt{1-\omega}$ and overlap for $|p| > p_\omega$. If $E_p = -ipJ$, all the four bands do not overlap for all values of $p \in \mathbb{R}$ and the zero point $\lambda = 0$ is always in the gap between the branches of the continuous spectrum.

The next result shows that if $p = 0$, then the spectral stability problem (3.2) admits the zero eigenvalue of quadruple multiplicity. The zero eigenvalue is determined by the symmetries of the nonlinear Dirac equations with respect to the spatial translation and the gauge rotation.

Proposition 3.2 *For every $\omega \in \Omega$ and $p = 0$, the stability problem* (3.2) *admits exactly two eigenvectors in $H^1(\mathbb{R})$ for the eigenvalue $\lambda = 0$ given by*

$$\mathbf{F}_t = \partial_x \mathbf{U}_\omega, \quad \mathbf{F}_g = i\sigma\mathbf{U}_\omega, \tag{3.7}$$

where $\mathbf{U}_\omega = (U_\omega, \bar{U}_\omega, \bar{U}_\omega, U_\omega)^t$. *For each eigenvector* $\mathbf{F}_{t,g}$, *there exists a generalized eigenvector* $\tilde{\mathbf{F}}_{t,g}$ *in* $H^1(\mathbb{R})$ *from solutions of the inhomogeneous problem*

$$(D_\omega + W_\omega)\mathbf{F} = i\sigma \mathbf{F}_{t,g}, \tag{3.8}$$

in fact, in the explicit form,

$$\tilde{\mathbf{F}}_t = i\omega x \sigma \mathbf{U}_\omega - \frac{1}{2}\tilde{\sigma}\mathbf{U}_\omega, \quad \tilde{\mathbf{F}}_g = \partial_\omega \mathbf{U}_\omega, \tag{3.9}$$

where $\tilde{\sigma} = diag(1, 1, -1, -1)$. *Moreover, if* $\langle \mathbf{F}_{t,g}, \sigma\tilde{\mathbf{F}}_{t,g}\rangle_{L^2} \neq 0$, *no solutions of the inhomogeneous problem*

$$(D_\omega + W_\omega)\mathbf{F} = i\sigma \tilde{\mathbf{F}}_{t,g} \tag{3.10}$$

exist in $H^1(\mathbb{R})$.

Proof Existence of the eigenvectors (3.7) follows from the two symmetries of the massive Dirac equations and is checked by elementary substitution as $(D_\omega + W_\omega)\mathbf{F}_{t,g} = \mathbf{0}$. Because $(D_\omega + W_\omega)$ is a self-adjoint operator of the fourth order and solutions of $(D_\omega + W_\omega)\mathbf{F} = \mathbf{0}$ have constant Wronskian determinant in x, there exist at most two spatially decaying solutions of these homogeneous equations, which means that the stability problem (3.2) with $p = 0$ admits exactly two eigenvectors in $H^1(\mathbb{R})$ for $\lambda = 0$. Since

$$\langle \mathbf{F}_{t,g}, \sigma \mathbf{F}_{t,g}\rangle_{L^2} = \langle \mathbf{F}_{t,g}, \sigma \mathbf{F}_{g,t}\rangle_{L^2} = 0$$

there exist solutions of the inhomogeneous problem (3.8) in $H^1(\mathbb{R})$. Existence of the generalized eigenvectors (3.9) is checked by elementary substitution. Finally, under the condition $\langle \mathbf{F}_{t,g}, \sigma\tilde{\mathbf{F}}_{t,g}\rangle_{L^2} \neq 0$, no solutions of the inhomogeneous problem (3.10) exist in $H^1(\mathbb{R})$ by Fredholm's alternative. □

Our main result is formulated in the following theorem. The theorem guarantees spectral instability of the line solitary waves with respect to the transverse perturbations of sufficiently large period both for the massive Thirring model and the massive Gross–Neveu model in two spatial dimensions.

Theorem 3.3 *For every* $\omega \in \Omega$, *there exists* $p_0 > 0$ *such that for every* p *in* $0 < |p| < p_0$, *the spectral stability problem* (3.2) *with either* (3.3) *or* (3.4) *admits at least one eigenvalue* λ *with* $\mathrm{Re}(\lambda) > 0$. *Moreover, up to a suitable normalization, as* $p \to 0$, *the corresponding eigenvector* $\mathbf{F}$ *converges in* $L^2(\mathbb{R})$ *to* $\mathbf{F}_t$ *for* (3.2) *and* (3.3) *and to* $\mathbf{F}_g$ *for* (3.2) *and* (3.4).

Simultaneously, there exists at least one pair of purely imaginary eigenvalues λ *of the spectral stability problem* (3.2), *and the corresponding eigenvector* $\mathbf{F}$ *converges as* $p \to 0$ *to the other eigenvector of Proposition* 3.2.

The proof of Theorem 3.3 is based on the perturbation theory for the Jordan block associated with the zero eigenvalue of the spectral problem (3.2) existing for $p = 0$, according to Proposition 3.2. The zero eigenvalue is isolated from the continuous spectrum, according to Proposition 3.1. Consequently, we do not have to deal with bifurcations from the continuous spectrum (unlike the difficult tasks of the recent work Boussaid and Comech 2012), but can develop straightforward perturbation expansions based on a modification of the Lyapunov–Schmidt reduction method.

A useful technical approach to the perturbation theory for the spectral stability problem (3.2) is based on the block diagonalization of the 4×4 matrix operator into two 2×2 Dirac operators. This block diagonalization technique was introduced in Chugunova and Pelinovsky (2006) and used for numerical approximations of eigenvalues of the spectral stability problem for the massive Dirac equations. After the block diagonalization, each Dirac operator has a one-dimensional kernel space induced by either translational or gauge symmetries. It enables us to uncouple the invariant subspaces associated with the Jordan block for the zero eigenvalue of the spectral stability problem (3.2) with $p = 0$.

Using the self-similarity transformation matrix

$$T = \frac{1}{\sqrt{2}} \begin{bmatrix} 1 & 0 & 1 & 0 \\ 0 & 1 & 0 & 1 \\ 0 & 1 & 0 & -1 \\ 1 & 0 & -1 & 0 \end{bmatrix}, \quad T^{-1} = \frac{1}{\sqrt{2}} \begin{bmatrix} 1 & 0 & 0 & 1 \\ 0 & 1 & 1 & 0 \\ 1 & 0 & 0 & -1 \\ 0 & 1 & -1 & 0 \end{bmatrix},$$

and setting $\mathbf{F} = T\mathbf{V}$, we can rewrite the spectral stability problem (3.2) in the following form:

$$i\lambda T^{-1}\sigma T\mathbf{V} = T^{-1}(D_\omega + E_p + W_\omega)T\mathbf{V}, \tag{3.11}$$

where

$$T^{-1}D_\omega T = \begin{bmatrix} -i\partial_x + \omega & -1 & 0 & 0 \\ -1 & i\partial_x + \omega & 0 & 0 \\ 0 & 0 & -i\partial_x + \omega & 1 \\ 0 & 0 & 1 & i\partial_x + \omega \end{bmatrix}, \quad T^{-1}\sigma T = \begin{bmatrix} 0 & 0 & 1 & 0 \\ 0 & 0 & 0 & -1 \\ 1 & 0 & 0 & 0 \\ 0 & -1 & 0 & 0 \end{bmatrix}, \tag{3.12}$$

whereas the transformation of matrices E_p and W_ω depend on the particular form of the nonlinear Dirac equations. For the model (2.2) with $\alpha_1 = 0$ and $\alpha_2 = 1$, we obtain

$$T^{-1}E_pT = p^2 \begin{bmatrix} 1 & 0 & 0 & 0 \\ 0 & 1 & 0 & 0 \\ 0 & 0 & 1 & 0 \\ 0 & 0 & 0 & 1 \end{bmatrix}, \quad T^{-1}W_\omega T = \begin{bmatrix} 2|U_\omega|^2 & U_\omega^2 & 0 & 0 \\ \overline{U}_\omega^2 & 2|U_\omega|^2 & 0 & 0 \\ 0 & 0 & 0 & -U_\omega^2 \\ 0 & 0 & -\overline{U}_\omega^2 & 0 \end{bmatrix}. \tag{3.13}$$

For the model (2.9) with $\beta_1 = -\beta_2 = \frac{1}{2}$, we obtain

$$T^{-1}E_pT = ip\begin{bmatrix} 0 & 0 & 0 & 1 \\ 0 & 0 & 1 & 0 \\ 0 & -1 & 0 & 0 \\ -1 & 0 & 0 & 0 \end{bmatrix},$$

$$T^{-1}W_\omega T = \begin{bmatrix} 2|U_\omega|^2 & U_\omega^2 + 3\bar{U}_\omega^2 & 0 & 0 \\ 3U_\omega^2 + \bar{U}_\omega^2 & 2|U_\omega|^2 & 0 & 0 \\ 0 & 0 & 0 & -U_\omega^2 - \bar{U}_\omega^2 \\ 0 & 0 & -U_\omega^2 - \bar{U}_\omega^2 & 0 \end{bmatrix}. \quad (3.14)$$

Let us apply the self-similarity transformation to the eigenvectors and generalized eigenvectors of Proposition 3.2. Using $\mathbf{F} = T\mathbf{V}$, the eigenvectors (3.7) become

$$\mathbf{V}_t = \begin{pmatrix} U_\omega' \\ \overline{U}_\omega' \\ 0 \\ 0 \end{pmatrix} \quad \text{and} \quad \mathbf{V}_g = i\begin{pmatrix} 0 \\ 0 \\ U_\omega \\ -\overline{U}_\omega \end{pmatrix}, \quad (3.15)$$

whereas the generalized eigenvectors (3.9) become

$$\tilde{\mathbf{V}}_t = i\omega x\begin{pmatrix} 0 \\ 0 \\ U_\omega \\ -\overline{U}_\omega \end{pmatrix} - \frac{1}{2}\begin{pmatrix} 0 \\ 0 \\ U_\omega \\ \overline{U}_\omega \end{pmatrix} \quad \text{and} \quad \tilde{\mathbf{V}}_g = \partial_\omega\begin{pmatrix} U_\omega \\ \overline{U}_\omega \\ 0 \\ 0 \end{pmatrix}. \quad (3.16)$$

Setting $\Phi_V = [\mathbf{V}_t, \mathbf{V}_g, \tilde{\mathbf{V}}_t, \tilde{\mathbf{V}}_g]$ and denoting $\mathcal{S} = T^{-1}\sigma T$, we compute elements of the matrix of skew-symmetric inner products between eigenvectors and generalized eigenvectors:

$$\langle \Phi_V, \mathcal{S}\Phi_V\rangle_{L^2} = \begin{bmatrix} 0 & 0 & \langle \mathbf{V}_t, \mathcal{S}\tilde{\mathbf{V}}_t\rangle_{L^2} & 0 \\ 0 & 0 & 0 & \langle \mathbf{V}_g, \mathcal{S}\tilde{\mathbf{V}}_g\rangle_{L^2} \\ \langle \tilde{\mathbf{V}}_t, \mathcal{S}\mathbf{V}_t\rangle_{L^2} & 0 & 0 & 0 \\ 0 & \langle \tilde{\mathbf{V}}_g, \mathcal{S}\mathbf{V}_g\rangle_{L^2} & 0 & 0 \end{bmatrix}, \quad (3.17)$$

where only nonzero elements are included. Verification of (3.17) is straightforward except for the term

$$\langle \tilde{\mathbf{V}}_t, \mathcal{S}\tilde{\mathbf{V}}_g\rangle_{L^2} = -i\omega\int_{\mathbb{R}} x\partial_\omega|U_\omega|^2 \mathrm{d}x - \frac{1}{2}\int_{\mathbb{R}}\left(\bar{U}_\omega\partial_\omega U_\omega - U_\omega\partial_\omega\bar{U}_\omega\right)\mathrm{d}x = 0. \quad (3.18)$$

Both integrals in (3.18) are zero because $x\partial_\omega |U_\omega|^2$ and $\mathrm{Im}(\bar{U}_\omega \partial_\omega U_\omega)$ are odd functions of x. As for the nonzero elements, we compute them explicitly from (3.15) and (3.16):

$$\langle \mathbf{V}_t, \mathcal{S}\tilde{\mathbf{V}}_t\rangle_{L^2} = -i\omega \int_{\mathbb{R}} |U_\omega|^2 \mathrm{d}x + \frac{1}{2}\int_{\mathbb{R}} \left(\bar{U}_\omega U'_\omega - U_\omega \bar{U}'_\omega\right) \mathrm{d}x \tag{3.19}$$

and

$$\langle \mathbf{V}_g, \mathcal{S}\tilde{\mathbf{V}}_g\rangle_{L^2} = -i\frac{\mathrm{d}}{\mathrm{d}\omega}\int_{\mathbb{R}} |U_\omega|^2 \mathrm{d}x. \tag{3.20}$$

Remark 4 In further analysis, we obtain explicit expressions for (3.19) and (3.20) and show that they are nonzero for every $\omega \in \Omega$. Consequently, the assumption $\langle \mathbf{F}_{t,g}, \sigma\tilde{\mathbf{F}}_{t,g}\rangle_{L^2} \neq 0$ in Proposition 3.2 is verified for either (3.3) or (3.4) in the spectral stability problem (3.2).

We shall now proceed separately with the proof of Theorem 3.3 for the massive Thirring and Gross–Neveu models in two spatial dimensions. Moreover, we derive explicit asymptotic expressions for the eigenvalues mentioned in Theorem 3.3.

3.1 Perturbation Theory for the Massive Thirring Model

The block-diagonalized system (3.11) with (3.12) and (3.13) can be rewritten in the explicit form

$$\begin{pmatrix} H_+ & 0 \\ 0 & H_- \end{pmatrix} \mathbf{V} + p^2 \begin{pmatrix} \sigma_0 & 0 \\ 0 & \sigma_0 \end{pmatrix} \mathbf{V} = i\lambda \begin{pmatrix} 0 & \sigma_3 \\ \sigma_3 & 0 \end{pmatrix} \mathbf{V}, \tag{3.21}$$

where

$$H_+ = \begin{pmatrix} -i\partial_x + \omega + 2|U_\omega|^2 & -1 + U_\omega^2 \\ -1 + \overline{U}_\omega^2 & i\partial_x + \omega + 2|U_\omega|^2 \end{pmatrix}, \quad H_- = \begin{pmatrix} -i\partial_x + \omega & 1 - U_\omega^2 \\ 1 - \overline{U}_\omega^2 & i\partial_x + \omega \end{pmatrix}, \tag{3.22}$$

and the following Pauli matrices are used throughout our work:

$$\sigma_0 = \begin{pmatrix} 1 & 0 \\ 0 & 1 \end{pmatrix}, \quad \sigma_1 = \begin{pmatrix} 0 & 1 \\ 1 & 0 \end{pmatrix}, \quad \sigma_3 = \begin{pmatrix} 1 & 0 \\ 0 & -1 \end{pmatrix}. \tag{3.23}$$

Note that H_+ and H_- are self-adjoint operators in $L^2(\mathbb{R}, \mathbb{C}^2)$ with the domain in $H^1(\mathbb{R}, \mathbb{C}^2)$. The operators $H_\pm$ satisfy the symmetry

$$\sigma_1 H_\pm = \bar{H}_\pm \sigma_1, \tag{3.24}$$

whereas the Pauli matrices satisfy the relation

$$\sigma_1\sigma_1 = \sigma_3\sigma_3 = \sigma_0, \quad \sigma_1\sigma_3 + \sigma_3\sigma_1 = 0, \tag{3.25}$$

Before proving the main result of the perturbation theory for the massive Thirring model in two spatial dimensions, we note the following elementary result.

Proposition 3.4 *For every $\omega \in (-1, 1)$ and every $p \in \mathbb{R}$, eigenvalues λ of the spectral problem (3.21) are symmetric about the real and imaginary axes in the complex plane.*

Proof It follows from symmetries (3.24) and (3.25) that if λ is an eigenvalue of the spectral problem (3.21) with the eigenvector $\mathbf{V} = (v_1, v_2, v_3, v_4)^t$, then $\bar{\lambda}$, $-\lambda$, and $-\bar{\lambda}$ are also eigenvalues of the same problem with the eigenvectors $(\bar{v}_2, \bar{v}_1, \bar{v}_4, \bar{v}_3)^t$, $(v_1, v_2, -v_3, -v_4)^t$, and $(\bar{v}_2, \bar{v}_1, -\bar{v}_4, -\bar{v}_3)^t$. Consequently, we have the following:

- if λ is a simple real nonzero eigenvalue, then the eigenvector $\mathbf{V}$ can be chosen to satisfy the reduction $v_1 = \bar{v}_2$, $v_3 = \bar{v}_4$, whereas $-\lambda$ is also an eigenvalue with the eigenvector $(v_1, v_2, -v_3, -v_4)^t = (\bar{v}_2, \bar{v}_1, -\bar{v}_4, -\bar{v}_3)^t$;
- if λ is a simple purely imaginary nonzero eigenvalue, then the eigenvector $\mathbf{V}$ can be chosen to satisfy the reduction $v_1 = \bar{v}_2$, $v_3 = -\bar{v}_4$, whereas $\bar{\lambda}$ is also an eigenvalue with the eigenvector $(\bar{v}_2, \bar{v}_1, \bar{v}_4, \bar{v}_3)^t = (v_1, v_2, -v_3, -v_4)^t$;
- if a simple eigenvalue λ occurs in the first quadrant, then the symmetry generates eigenvalues in all other quadrants and all four eigenvectors generated by the symmetry are linearly independent.

The symmetry between eigenvalues also applies to multiple nonzero eigenvalues and the corresponding eigenvectors of the associated Jordan blocks. ◻

For the sake of simplicity, we denote

$$\mathcal{H} = \begin{pmatrix} H_+ & 0 \\ 0 & H_- \end{pmatrix}, \quad \mathcal{I} = \begin{pmatrix} \sigma_0 & 0 \\ 0 & \sigma_0 \end{pmatrix}, \quad \mathcal{S} = \begin{pmatrix} 0 & \sigma_3 \\ \sigma_3 & 0 \end{pmatrix}.$$

It follows from Proposition 3.2 and the explicit expressions (3.15) and (3.16) that

$$\mathcal{H}\mathbf{V}_{t,g} = \mathbf{0}, \quad \mathcal{H}\tilde{\mathbf{V}}_{t,g} = i\mathcal{S}\mathbf{V}_{t,g}. \tag{3.26}$$

Setting $\Phi_V = [\mathbf{V}_t, \mathbf{V}_g, \tilde{\mathbf{V}}_t, \tilde{\mathbf{V}}_g]$ as earlier, we note that

$$\langle \Phi_V, \mathcal{I}\Phi_V \rangle_{L^2} = \begin{bmatrix} \|\mathbf{V}_t\|_{L^2}^2 & 0 & 0 & 0 \\ 0 & \|\mathbf{V}_g\|_{L^2}^2 & 0 & 0 \\ 0 & 0 & \|\tilde{\mathbf{V}}_t\|_{L^2}^2 & 0 \\ 0 & 0 & 0 & \|\tilde{\mathbf{V}}_g\|_{L^2}^2 \end{bmatrix}, \tag{3.27}$$

where only nonzero terms are included. Again, it is straightforward to verify (3.27) from (3.15) and (3.16), except for the elements

$$\langle \mathbf{V}_t, \tilde{\mathbf{V}}_g \rangle_{L^2} = \int_{\mathbb{R}} \left(\bar{U}'_\omega \partial_\omega U_\omega + U'_\omega \partial_\omega \bar{U}_\omega \right) \mathrm{d}x = 0$$

and

$$\langle \mathbf{V}_g, \tilde{\mathbf{V}}_t \rangle_{L^2} = 2\omega \int_{\mathbb{R}} x|U_\omega|^2 \mathrm{d}x = 0.$$

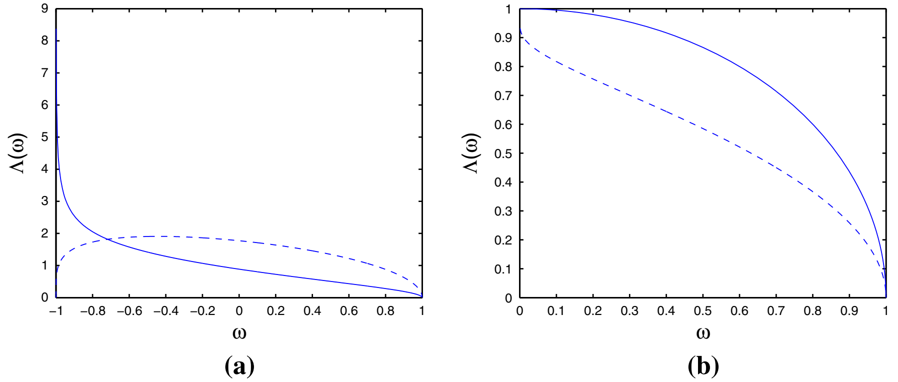

Fig. 1 Asymptotic expressions Λ_r (*solid line*) and Λ_i (*dashed line*) versus parameter ω for the massive Thirring (*left*) and Gross–Neveu (*right*) models

These elements are zero because $x|U_\omega|^2$ and $\mathrm{Re}(\bar{U}'_\omega \partial_\omega U_\omega)$ are odd functions of x.

The following result gives the outcome of the perturbation theory associated with the generalized null space of the spectral stability problem (3.21). The result is equivalent to the part of Theorem 3.3 corresponding to the spectral stability problem (3.2) with (3.3). The asymptotic expressions Λ_r and Λ_i of the real and imaginary eigenvalues λ at the leading order in p versus parameter ω are shown in Fig. 1a.

Lemma 3.5 *For every $\omega \in (-1, 1)$, there exists $p_0 > 0$ such that for every p with $0 < |p| < p_0$, the spectral stability problem* (3.21) *admits a pair of real eigenvalues λ with the eigenvectors $\mathbf{V} \in H^1(\mathbb{R})$ such that*

$$\lambda = \pm p\Lambda_r(\omega) + \mathcal{O}(p^3), \quad \mathbf{V} = \mathbf{V}_t \pm p\Lambda_r(\omega)\tilde{\mathbf{V}}_t + \mathcal{O}_{H^1}(p^2) \quad as \quad p \to 0, \tag{3.28}$$

where $\Lambda_r = (1-\omega^2)^{-1/4}\|U'_\omega\|_{L^2} > 0$. Simultaneously, it admits a pair of purely imaginary eigenvalues λ with the eigenvector $\mathbf{V} \in H^1(\mathbb{R})$ such that

$$\lambda = \pm ip\Lambda_i(\omega) + \mathcal{O}(p^3), \quad \mathbf{V} = \mathbf{V}_g \pm ip\Lambda_i(\omega)\tilde{\mathbf{V}}_g + \mathcal{O}_{H^1}(p^2) \quad as \quad p \to 0, \tag{3.29}$$

where $\Lambda_i = \sqrt{2}(1-\omega^2)^{1/4}\|U_\omega\|_{L^2} > 0$.

Before proving Lemma 3.5, we give formal computations of the perturbation theory, which recover expansions (3.28) and (3.29) with explicit expressions for $\Lambda_r(\omega)$ and $\Lambda_i(\omega)$. Consider the following formal expansions

$$\lambda = p\Lambda_1 + p^2\Lambda_2 + \mathcal{O}(p^3), \quad \mathbf{V} = \mathbf{V}_0 + p\Lambda_1\mathbf{V}_1 + p^2\mathbf{V}_2 + \mathcal{O}_{H^1}(p^3), \tag{3.30}$$

where $\mathbf{V}_0$ is spanned by the eigenvectors (3.15), $\mathbf{V}_1$ is spanned by the generalized eigenvectors (3.16), and $\mathbf{V}_2$ satisfies the linear inhomogeneous equation

$$\mathcal{H}\mathbf{V}_2 = -\mathcal{I}\mathbf{V}_0 + i\Lambda_1^2\mathcal{S}\mathbf{V}_1 + i\Lambda_2\mathcal{S}\mathbf{V}_0. \tag{3.31}$$

By Fredholm's alternative, there exists a solution $\mathbf{V}_2 \in H^1(\mathbb{R})$ of the linear inhomogeneous equation (3.31) if and only if Λ_1 is found from the quadratic equation

$$i\Lambda_1^2\langle \mathbf{W}_0, \mathcal{S}\mathbf{V}_1\rangle_{L^2} = \langle \mathbf{W}_0, \mathbf{V}_0\rangle_{L^2}, \tag{3.32}$$

where $\mathbf{W}_0$ is spanned by the eigenvectors (3.15) independently of $\mathbf{V}_0$. Because of the block diagonalization of the projection matrices in (3.17) and (3.27), the 2-by-2 matrix eigenvalue problem (3.32) is diagonal and we can proceed separately with precise computations for each eigenvector in $\mathbf{V}_0$.

Selecting $\mathbf{V}_0 = \mathbf{W}_0 = \mathbf{V}_t$ and $\mathbf{V}_1 = \tilde{\mathbf{V}}_t$, we rewrite the solvability condition (3.32) as the following quadratic equation

$$\Lambda_1^2 \int_{\mathbb{R}} \left(\omega|U_\omega|^2 + \frac{i}{2}\left(\bar{U}_\omega U_\omega' - U_\omega \bar{U}_\omega'\right)\right) \mathrm{d}x = 2\int_{\mathbb{R}} |U_\omega'|^2 \mathrm{d}x,$$

where we have used relation (3.19). Substituting the exact expression (2.7), we obtain

$$\int_{\mathbb{R}} \left(\omega|U_\omega|^2 + \frac{i}{2}\left(\bar{U}_\omega U_\omega' - U_\omega \bar{U}_\omega'\right)\right) \mathrm{d}x = 2\sqrt{1-\omega^2} \tag{3.33}$$

and

$$\int_{\mathbb{R}} |U_\omega'|^2 \mathrm{d}x = -4\omega\sqrt{1-\omega^2} + 4(1+\omega^2)\arctan\left(\sqrt{\frac{1-\omega}{1+\omega}}\right),$$

which yields the expression $\Lambda_1^2 = (1-\omega^2)^{-1/2}\|U_\omega'\|_{L^2}^2 = \Lambda_r(\omega)^2$.

Selecting now $\mathbf{V}_0 = \mathbf{W}_0 = \mathbf{V}_g$ and $\mathbf{V}_1 = \tilde{\mathbf{V}}_g$, we rewrite the solvability condition (3.32) as the following quadratic equation

$$\Lambda_1^2 \frac{\mathrm{d}}{\mathrm{d}\omega}\int_{\mathbb{R}} |U_\omega|^2 \mathrm{d}x = 2\int_{\mathbb{R}} |U_\omega|^2 \mathrm{d}x,$$

where we have used relation (3.20). Substituting the exact expression (2.7), we obtain

$$\int_{\mathbb{R}} |U_\omega|^2 \mathrm{d}x = 4\arctan\left(\sqrt{\frac{1-\omega}{1+\omega}}\right)$$

and

$$\frac{\mathrm{d}}{\mathrm{d}\omega}\int_{\mathbb{R}} |U_\omega|^2 \mathrm{d}x = -\frac{1}{\sqrt{1-\omega^2}}, \tag{3.34}$$

which yields the expression for $\Lambda_1^2 = -2(1-\omega^2)^{1/2}\|U_\omega\|_{L^2}^2 = -\Lambda_i(\omega)^2$. Note that the nonzero values in (3.33) and (3.34) verify the nonzero values in (3.19) and (3.20), and hence, the assumption $\langle \mathbf{F}_{t,g}, \sigma\tilde{\mathbf{F}}_{t,g}\rangle_{L^2} \neq 0$ in Proposition 3.2, according to Remark 4.

We shall now justify the asymptotic expansions (3.28) and (3.29) to give the proof of Lemma 3.5. Note that Λ_2 in (3.30) is not determined in the linear equation (3.31). Nevertheless, we will show in the proof of Lemma 3.5 that $\Lambda_2 = 0$, see (3.36), (3.44), and (3.46) below.

Proof of Lemma 3.5 Consider the linearized operator for the spectral problem (3.21):

$$\mathcal{A}_{\lambda,p} = \mathcal{H} + p^2\mathcal{I} - i\lambda\mathcal{S} : H^1(\mathbb{R}) \to L^2(\mathbb{R}).$$

This operator is self-adjoint if $\lambda \in i\mathbb{R}$ and non-self-adjoint if $\lambda \notin i\mathbb{R}$.

Since $\mathcal{S}\mathcal{S} = \mathcal{I}$, it follows from Proposition 3.2 and the computations (3.26) that $\mathcal{S}\mathcal{H}$ has the four-dimensional generalized null space $X_0 \subset L^2(\mathbb{R})$ spanned by the vectors in Φ_V. By Propositions 3.1, the rest of spectrum of $\mathcal{S}\mathcal{H}$ is bounded away from zero. By Fredholm's theory, the range of $\mathcal{S}\mathcal{H}$ is orthogonal with respect to the generalized null space $Y_0 \subset L^2(\mathbb{R})$ of the adjoint operator $\mathcal{H}\mathcal{S}$, which is spanned by the vectors in $\mathcal{S}\Phi_V$.

The inhomogeneous equation $(\mathcal{H} - i\lambda\mathcal{S})g = f$ for $f \in L^2(\mathbb{R})$ is equivalent to the inhomogeneous equation $(\mathcal{S}\mathcal{H} - i\lambda)g = \mathcal{S}f$. By Fredholm's alternative, for $\lambda = 0$, a solution $g \in H^1(\mathbb{R})$ exists if and only if $\mathcal{S}f$ is orthogonal to the generalized kernel of $\mathcal{H}\mathcal{S}$, which means that $\mathcal{S}f \in Y_0^\perp$ or equivalently, $f \in X_0^\perp$. For $\lambda \neq 0$ but small, it is natural to define the solution $g \in H^1(\mathbb{R})$ uniquely by the constraint $g \in Y_0^\perp$.

Consequently, there is $\lambda_0 > 0$ sufficiently small such that $\mathcal{A}_{\lambda,0}$ with $|\lambda| < \lambda_0$ is invertible on $X_0^\perp$ with a bounded inverse in $Y_0^\perp$. Since $p^2\mathcal{I}$ is a bounded self-adjoint perturbation to $\mathcal{H}$, there exist positive constants λ_0, p_0, and C_0 such that for all $|\lambda| < \lambda_0$, $|p| < p_0$, and all $\mathbf{f} \in X_0^\perp \subset L^2(\mathbb{R})$, there exists a unique $\mathcal{A}_{\lambda,p}^{-1}\mathbf{f} \in Y_0^\perp$ satisfying

$$\|\mathcal{A}_{\lambda,p}^{-1}\mathbf{f}\|_{L^2} \leq C_0\|\mathbf{f}\|_{L^2}. \tag{3.35}$$

Moreover, $\mathcal{A}_{\lambda,p}^{-1}\mathbf{f} \in H^1(\mathbb{R})$.

Let us now use the method of the Lyapunov–Schmidt reduction. We apply the partition of Φ_V as $\Phi_V^{(0)} = [\mathbf{V}_t, \mathbf{V}_g]$ and $\Phi_V^{(1)} = [\tilde{\mathbf{V}}_t, \tilde{\mathbf{V}}_g]$. Given the computations above, we consider the decomposition of the solution of the spectral problem (3.21) in the form

$$\begin{cases} \lambda = p(\Lambda + \mu_p), \\ \mathbf{V} = \Phi_V^{(0)}\boldsymbol{\alpha}_p + p\Phi_V^{(1)}((\Lambda + \mu_p)\boldsymbol{\alpha}_p + \boldsymbol{\gamma}_p) + \mathbf{V}_p, \end{cases} \tag{3.36}$$

where $\Lambda \in \mathbb{C}$ is p-independent, whereas $\mu_p \in \mathbb{C}$, $\boldsymbol{\alpha}_p \in \mathbb{C}^2$, $\boldsymbol{\gamma}_p \in \mathbb{C}^2$, and $\mathbf{V}_p \in H^1(\mathbb{R})$ may depend on p. For uniqueness of the decomposition, we use the Fredholm theory and require that the correction term $\mathbf{V}_p$ satisfies the orthogonality conditions:

$$\langle \Phi_V, \mathcal{S}\mathbf{V}_p \rangle_{L^2} = 0, \tag{3.37}$$

which ensures that $\mathbf{V}_p \in H^1(\mathbb{R}) \cap Y_0^\perp$. Substituting expansions (3.36) into the spectral problem (3.21), we obtain

$$\begin{aligned}\left(\mathcal{H} + p^2\mathcal{I} - ip(\Lambda + \mu_p)\mathcal{S}\right)\mathbf{V}_p + p^2\left(\Phi_V^{(0)}\boldsymbol{\alpha}_p + p\Phi_V^{(1)}((\Lambda + \mu_p)\boldsymbol{\alpha}_p + \boldsymbol{\gamma}_p)\right) \\ = ip^2(\Lambda + \mu_p)\mathcal{S}\Phi_V^{(1)}((\Lambda + \mu_p)\boldsymbol{\alpha}_p + \boldsymbol{\gamma}_p) - ip\mathcal{S}\Phi_V^{(0)}\boldsymbol{\gamma}_p. \end{aligned} \tag{3.38}$$

In order to solve Eq. (3.38) for $\mathbf{V}_p$ in $H^1(\mathbb{R}) \cap Y_0^\perp$, we project the equation to $X_0^\perp$. It makes sense to do so separately for $\Phi_V^{(0)}$ and $\Phi_V^{(1)}$. Using the projection matrices (3.17) and (3.27) as well as the orthogonality conditions (3.37), we obtain

$$\begin{aligned} p^2\left\langle \Phi_V^{(0)}, \mathbf{V}_p \right\rangle_{L^2} + p^2\left\langle \Phi_V^{(0)}, \Phi_V^{(0)} \right\rangle_{L^2}\boldsymbol{\alpha}_p \\ = ip^2(\Lambda + \mu_p)\left\langle \Phi_V^{(0)}, \mathcal{S}\Phi_V^{(1)} \right\rangle_{L^2}((\Lambda + \mu_p)\boldsymbol{\alpha}_p + \boldsymbol{\gamma}_p) \end{aligned} \tag{3.39}$$

and

$$\begin{aligned} p^2\left\langle \Phi_V^{(1)}, \mathbf{V}_p \right\rangle_{L^2} + p^3\left\langle \Phi_V^{(1)}, \Phi_V^{(1)} \right\rangle_{L^2}((\Lambda + \mu_p)\boldsymbol{\alpha}_p + \boldsymbol{\gamma}_p) \\ = -ip\left\langle \Phi_V^{(1)}, \mathcal{S}\Phi_V^{(0)} \right\rangle_{L^2}\boldsymbol{\gamma}_p. \end{aligned} \tag{3.40}$$

Under the constraints (3.39) and (3.40), the right-hand side of Eq. (3.38) belongs to $X_0^\perp$. The resolvent estimate (3.35) implies that the operator $A_{\lambda,p}$ can be inverted with a bounded inverse in $Y_0^\perp$. By the inverse function theorem, there are positive numbers $p_1 \leq p_0$, μ_1, and C_1 such that for every $|p| < p_1$ and $|\mu_p| < \mu_1$, there exists a unique solution of Eq. (3.38) for $\mathbf{V}_p$ in $H^1(\mathbb{R}) \cap Y_0^\perp$ satisfying the estimate

$$\|\mathbf{V}_p\|_{L^2} \leq C_1\left(p^2\|\boldsymbol{\alpha}_p\| + |p|\|\boldsymbol{\gamma}_p\|\right). \tag{3.41}$$

Substituting this solution to the projection equations (3.39) and (3.40), we shall be looking for values of Λ, μ_p, $\boldsymbol{\alpha}_p$, and $\boldsymbol{\gamma}_p$ for $|p| < p_1$ sufficiently small. Using the estimate (3.41), we realize that the leading order of Eq. (3.39) is

$$\left\langle \Phi_V^{(0)}, \Phi_V^{(0)} \right\rangle_{L^2}\mathbf{c} = i\Lambda^2\left\langle \Phi_V^{(0)}, \mathcal{S}\Phi_V^{(1)} \right\rangle_{L^2}\mathbf{c}, \quad \mathbf{c} \in \mathbb{C}^2. \tag{3.42}$$

This equation is diagonal and admits two eigenvalues for Λ^2 given by $\Lambda_r(\omega)^2$ and $-\Lambda_i(\omega)^2$, so that

$$\|\mathbf{V}_t\|_{L^2}^2 = i\Lambda_r(\omega)^2\langle \mathbf{V}_t, \mathcal{S}\tilde{\mathbf{V}}_t \rangle_{L^2}, \quad \|\mathbf{V}_g\|_{L^2}^2 = -i\Lambda_i(\omega)^2\langle \mathbf{V}_g, \mathcal{S}\tilde{\mathbf{V}}_g \rangle_{L^2}.$$

Choosing Λ^2 being equal to one of the two eigenvalues (which are distinct), we obtain a rank-one coefficient matrix for Eq. (3.39) at the leading order. In what follows, we omit the argument ω from Λ_r and Λ_i.

For simplicity, let us choose $\Lambda^2 = \Lambda_r^2$ (the other case is considered similarly) and represent $\boldsymbol{\alpha}_p = (\alpha_p, \beta_p)^t$ and $\boldsymbol{\gamma}_p = (\gamma_p, \delta_p)^t$. In this case, α_p can be normalized to unity independently of p, after which Eq. (3.39) divided by p^2 is rewritten in the following explicit form

$$\begin{bmatrix} \|\mathbf{V}_t\|^2_{L^2} & 0 \\ 0 & \|\mathbf{V}_g\|^2_{L^2} \end{bmatrix} \begin{bmatrix} \left(1+\frac{\mu_p}{\Lambda_r}\right)^2 - 1 + \frac{\Lambda_r+\mu_p}{\Lambda_r^2}\gamma_p \\ -\frac{\Lambda_r^2}{\Lambda_i^2}\left(1+\frac{\mu_p}{\Lambda_r}\right)^2\beta_p - \beta_p - \frac{\Lambda_r+\mu_p}{\Lambda_i^2}\delta_p \end{bmatrix} = \left\langle \Phi_V^{(0)}, \mathbf{V}_p \right\rangle_{L^2}. \tag{3.43}$$

We invoke the implicit function theorem for vector functions. It follows from the estimate (3.41) that there are positive numbers $p_2 \leq p_1$ and C_2 such that for every $|p| < p_2$, there exists a unique solution of Eq. (3.43) for μ_p and β_p satisfying the estimate

$$|\mu_p| + |\beta_p| \leq C_2 \left(\|\boldsymbol{\gamma}_p\| + \|\mathbf{V}_p\|_{L^2}\right) \leq C_2 \left(\|\boldsymbol{\gamma}_p\| + p^2\right), \tag{3.44}$$

where the last inequality with a modified value of constant C_2 is due to the estimate (3.41).

Finally, we divide Eq. (3.40) by p and rewrite it in the form

$$-i\left\langle \Phi_V^{(1)}, \mathcal{S}\Phi_V^{(0)} \right\rangle_{L^2} \boldsymbol{\gamma}_p = p\left\langle \Phi_V^{(1)}, \mathbf{V}_p \right\rangle_{L^2} + p^2\left\langle \Phi_V^{(1)}, \Phi_V^{(1)} \right\rangle_{L^2}((\Lambda+\mu_p)\boldsymbol{\alpha}_p + \boldsymbol{\gamma}_p). \tag{3.45}$$

Thanks to the estimates (3.41) and (3.44), Eq. (3.45) can be solved for $\boldsymbol{\gamma}_p$ by the implicit function theorem, if p is sufficiently small and $\mathbf{V}_p$, μ_p, and $\boldsymbol{\alpha}_p$ are substituted from solutions of the previous equations. As a result, there are positive numbers $p_3 \leq p_2$ and C_3 such that for every $|p| < p_3$, there exists a unique solution of Eq. (3.45) for $\boldsymbol{\gamma}_p$ satisfying the estimate

$$\|\boldsymbol{\gamma}_p\| \leq C_3 \left(p^2 + p\|\mathbf{V}_p\|_{L^2}\right) \leq C_3 p^2, \tag{3.46}$$

where the last inequality with a modified value of constant C_3 is due to the estimate (3.41).

Decomposition (3.36) and estimates (3.41), (3.44), and (3.46) justify the asymptotic expansion (3.28). It remains to prove that the eigenvalue $\lambda = p(\Lambda_r + \mu_p)$ is purely real. Since Λ_r is real, the result holds if μ_p is real. Assume that μ_p has a nonzero imaginary part. By Proposition 3.4, there exists another distinct eigenvalue of the spectral problem (3.21) given by $\lambda = (p\Lambda_r + \bar{\mu}_p)$ such that $\bar{\mu}_p = \mathcal{O}(p^2)$ as $p \to 0$. However, the existence of this distinct eigenvalue contradicts the uniqueness of constructing of μ_p and all terms in the decomposition (3.36). Therefore, $\bar{\mu}_p = \mu_p$, so that $\lambda = p(\Lambda_r + \mu_p)$ is real.

The asymptotic expansion (3.29) is proved similarly with the normalization $\beta_p = 1$ and the choice $\Lambda^2 = -\Lambda_i^2$ among eigenvalues of the reduced eigenvalue problem (3.42). □

3.2 Perturbation Theory for the Massive Gross–Neveu Model

The block-diagonalized system (3.11) with (3.12) and (3.14) can be rewritten in the explicit form

$$\begin{pmatrix} H_+ & 0 \\ 0 & H_- \end{pmatrix} \mathbf{V} + ip \begin{pmatrix} 0 & \sigma_1 \\ -\sigma_1 & 0 \end{pmatrix} \mathbf{V} = i\lambda \begin{pmatrix} 0 & \sigma_3 \\ \sigma_3 & 0 \end{pmatrix} \mathbf{V}, \tag{3.47}$$

where σ_1 and σ_3 are the Pauli matrices, whereas

$$H_+ = \begin{pmatrix} -i\partial_x + \omega + 2|U_\omega|^2 & -1 + U_\omega^2 + 3\overline{U}_\omega^2 \\ -1 + \overline{U}_\omega^2 + 3U_\omega^2 & i\partial_x + \omega + 2|U_\omega|^2 \end{pmatrix} \quad \text{and}$$
$$H_- = \begin{pmatrix} -i\partial_x + \omega & 1 - U_\omega^2 - \overline{U}_\omega^2 \\ 1 - U_\omega^2 - \overline{U}_\omega^2 & i\partial_x + \omega \end{pmatrix}.$$

We note again the symmetry relation (3.24), which applies to the Dirac operators $H_\pm$ for the massive Gross–Neveu model as well. From this symmetry, we derive the result, which is similar to Proposition 3.4 and is proved directly.

Proposition 3.6 *For every $\omega \in (0, 1)$, if λ is an eigenvalue of the spectral problem* (3.47) *with $p \in \mathbb{R}$ and the eigenvector $\mathbf{V} = (v_1, v_2, v_3, v_4)^t$, then $-\bar{\lambda}$ is also an eigenvalue of the same problem with the eigenvector $(\bar{v}_2, \bar{v}_1, -\bar{v}_4, -\bar{v}_3)^t$, whereas $\bar{\lambda}$ and $-\lambda$ are eigenvalues of the spectral problem* (3.47) *with $-p \in \mathbb{R}$ and the eigenvectors $(\bar{v}_2, \bar{v}_1, \bar{v}_4, \bar{v}_3)^t$ and $(v_1, v_2, -v_3, -v_4)^t$, respectively. Consequently, for every $p \in \mathbb{R}$, eigenvalues λ of the spectral problem* (3.47) *are symmetric about the imaginary axis.*

For the sake of simplicity, we use again the notations

$$\mathcal{H} = \begin{pmatrix} H_+ & 0 \\ 0 & H_- \end{pmatrix}, \quad \mathcal{P} = i \begin{pmatrix} 0 & \sigma_1 \\ -\sigma_1 & 0 \end{pmatrix}, \quad \mathcal{S} = \begin{pmatrix} 0 & \sigma_3 \\ \sigma_3 & 0 \end{pmatrix}.$$

The relations (3.26) hold true for this case as well. Besides the eigenvectors (3.15) and the generalized eigenvectors (3.16), we need solutions of the linear inhomogeneous equations

$$\mathcal{H}\mathbf{V} = -\mathcal{P}\mathbf{V}_{t,g}, \tag{3.48}$$

which are given by

$$\check{\mathbf{V}}_t = -\frac{1}{2}\begin{pmatrix} 0 \\ 0 \\ \overline{U}_\omega \\ -U_\omega \end{pmatrix} \quad \text{and} \quad \check{\mathbf{V}}_g = -\frac{1}{2\omega}\begin{pmatrix} \overline{U}_\omega \\ -U_\omega \\ 0 \\ 0 \end{pmatrix}. \tag{3.49}$$

The existence of these explicit expressions is checked by elementary substitution.

We apply again the partition of Φ_V as $\Phi_V^{(0)} = [\mathbf{V}_t, \mathbf{V}_g]$ and $\Phi_V^{(1)} = [\tilde{\mathbf{V}}_t, \tilde{\mathbf{V}}_g]$. In addition, we augment the matrix Φ_V with $\Phi_V^{(2)} = [\check{\mathbf{V}}_t, \check{\mathbf{V}}_g]$ and compute the missing entries in the projection matrices:

$$\left\langle \Phi_V^{(0)}, \mathcal{S}\Phi_V^{(2)} \right\rangle_{L^2} = \left\langle \Phi_V^{(2)}, \mathcal{S}\Phi_V^{(2)} \right\rangle_{L^2} = \begin{bmatrix} 0 & 0 \\ 0 & 0 \end{bmatrix}, \tag{3.50}$$

and

$$\left\langle \Phi_V^{(1)}, \mathcal{S}\Phi_V^{(2)} \right\rangle_{L^2} = \begin{bmatrix} 0 & 0 \\ \langle \tilde{\mathbf{V}}_g, \mathcal{S}\check{\mathbf{V}}_t \rangle_{L^2} & 0 \end{bmatrix}. \tag{3.51}$$

Indeed, in addition to the matrix elements, which are trivially zero, we check that

$$\langle \mathbf{V}_g, \mathcal{S}\check{\mathbf{V}}_g \rangle_{L^2} = \frac{i}{2\omega}\int_{\mathbb{R}} \left(\bar{U}_\omega^2 - U_\omega^2\right) \mathrm{d}x = 0, \tag{3.52}$$

because $\mathrm{Im}(U_\omega^2)$ is an odd function of x, and

$$\langle \tilde{\mathbf{V}}_t, \mathcal{S}\check{\mathbf{V}}_g \rangle_{L^2} = \frac{i}{2}\int_{\mathbb{R}} x \left(\bar{U}_\omega^2 - U_\omega^2\right) \mathrm{d}x + \frac{1}{4\omega}\int_{\mathbb{R}} (\bar{U}_\omega^2 + U_\omega^2) \mathrm{d}x = 0, \tag{3.53}$$

where the exact expression (2.11) is used. On the other hand, we have

$$\begin{aligned} \langle \tilde{\mathbf{V}}_g, \mathcal{S}\check{\mathbf{V}}_t \rangle_{L^2} &= -\frac{1}{4}\frac{\mathrm{d}}{\mathrm{d}\omega}\int_{\mathbb{R}} \left(\bar{U}_\omega^2 + U_\omega^2\right) \mathrm{d}x \\ &= -\frac{1}{2}\frac{\mathrm{d}}{\mathrm{d}\omega}\log\left(\frac{1+\omega+\sqrt{1-\omega^2}}{1+\omega-\sqrt{1-\omega^2}}\right) = \frac{1}{2\omega\sqrt{1-\omega^2}}, \end{aligned} \tag{3.54}$$

which is nonzero.

Similarly, we compute the zero projection matrices

$$\left\langle \Phi_V^{(0)}, \mathcal{P}\Phi_V^{(0)} \right\rangle_{L^2} = \left\langle \Phi_V^{(0)}, \mathcal{P}\Phi_V^{(1)} \right\rangle_{L^2} = \left\langle \Phi_V^{(1)}, \mathcal{P}\Phi_V^{(2)} \right\rangle_{L^2} = \begin{bmatrix} 0 & 0 \\ 0 & 0 \end{bmatrix} \tag{3.55}$$

and the nonzero projection matrices

$$\left\langle \Phi_V^{(1)}, \mathcal{P}\Phi_V^{(1)} \right\rangle_{L^2} = \begin{bmatrix} 0 & \langle \tilde{\mathbf{V}}_t, \mathcal{P}\tilde{\mathbf{V}}_g \rangle_{L^2} \\ \langle \tilde{\mathbf{V}}_g, \mathcal{P}\tilde{\mathbf{V}}_t \rangle_{L^2} & 0 \end{bmatrix}, \tag{3.56}$$

$$\left\langle \Phi_V^{(0)}, \mathcal{P}\Phi_V^{(2)} \right\rangle_{L^2} = \begin{bmatrix} \langle \mathbf{V}_t, \mathcal{P}\check{\mathbf{V}}_t \rangle_{L^2} & 0 \\ 0 & \langle \mathbf{V}_g, \mathcal{P}\check{\mathbf{V}}_g \rangle_{L^2} \end{bmatrix}, \tag{3.57}$$

and

$$\left\langle \Phi_V^{(2)}, \mathcal{P}\Phi_V^{(2)} \right\rangle_{L^2} = \begin{bmatrix} 0 & \langle \check{\mathbf{V}}_t, \mathcal{P}\check{\mathbf{V}}_g \rangle_{L^2} \\ \langle \check{\mathbf{V}}_g, \mathcal{P}\check{\mathbf{V}}_t \rangle_{L^2} & 0 \end{bmatrix}. \tag{3.58}$$

Indeed, the first matrix in (3.55) is zero because the Fredholm conditions for the inhomogeneous linear systems (3.48) are satisfied. The second matrix in (3.55) is zero because

$$\langle \mathbf{V}_t, \mathcal{P}\tilde{\mathbf{V}}_t \rangle_{L^2} = \frac{\omega}{2} \int_{\mathbb{R}} \left(U_\omega^2 - \bar{U}_\omega^2 \right) \mathrm{d}x = 0 \tag{3.59}$$

and

$$\langle \mathbf{V}_g, \mathcal{P}\tilde{\mathbf{V}}_g \rangle_{L^2} = \frac{1}{2} \frac{\mathrm{d}}{\mathrm{d}\omega} \int_{\mathbb{R}} \left(U_\omega^2 - \bar{U}_\omega^2 \right) \mathrm{d}x = 0. \tag{3.60}$$

The third matrix in (3.55) is zero because

$$\langle \tilde{\mathbf{V}}_t, \mathcal{P}\check{\mathbf{V}}_g \rangle_{L^2} = -\int_{\mathbb{R}} x |U_\omega|^2 \mathrm{d}x = 0 \tag{3.61}$$

and

$$\langle \tilde{\mathbf{V}}_g, \mathcal{P}\check{\mathbf{V}}_t \rangle_{L^2} = \frac{i}{2} \int_{\mathbb{R}} \left(U_\omega \partial_\omega \bar{U}_\omega - \bar{U}_\omega \partial_\omega U_\omega \right) \mathrm{d}x = 0. \tag{3.62}$$

For the projection matrices (3.56), (3.57), and (3.58), we compute the nonzero elements explicitly:

$$\langle \tilde{\mathbf{V}}_t, \mathcal{P}\tilde{\mathbf{V}}_g \rangle_{L^2} = \frac{i}{4} \frac{\mathrm{d}}{\mathrm{d}\omega} \int_{\mathbb{R}} \left(U_\omega^2 + \bar{U}_\omega^2 \right) \mathrm{d}x + \frac{\omega}{2} \frac{\mathrm{d}}{\mathrm{d}\omega} \int_{\mathbb{R}} x \left(U_\omega^2 - \bar{U}_\omega^2 \right) \mathrm{d}x, \tag{3.63}$$

$$\langle \mathbf{V}_t, \mathcal{P}\check{\mathbf{V}}_t \rangle_{L^2} = \frac{i}{2} \int_{\mathbb{R}} \left(U_\omega \bar{U}_\omega' - \bar{U}_\omega U_\omega' \right) \mathrm{d}x, \tag{3.64}$$

$$\langle \mathbf{V}_g, \mathcal{P}\check{\mathbf{V}}_g \rangle_{L^2} = -\frac{1}{\omega} \int_{\mathbb{R}} |U_\omega|^2 \mathrm{d}x, \tag{3.65}$$

$$\langle \check{\mathbf{V}}_t, \mathcal{P}\check{\mathbf{V}}_g \rangle_{L^2} = \frac{i}{4\omega} \int_{\mathbb{R}} \left(U_\omega^2 + \bar{U}_\omega^2 \right) \mathrm{d}x. \tag{3.66}$$

The following result gives the outcome of the perturbation theory associated with the generalized null space of the spectral stability problem (3.47). The result is equivalent to the part of Theorem 3.3 corresponding to the spectral stability problem (3.2) with (3.4). The asymptotic expressions Λ_r and Λ_i for the corresponding eigenvalues λ at the leading order in p versus parameter ω are shown in Fig. 1b.

Lemma 3.7 *For every $\omega \in (0, 1)$, there exists $p_0 > 0$ such that for every p with $0 < |p| < p_0$, the spectral stability problem (3.47) admits a pair of purely imaginary eigenvalues λ with the eigenvectors $\mathbf{V} \in H^1(\mathbb{R})$ such that*

$$\lambda = \pm i p \Lambda_i(\omega) + \mathcal{O}(p^3), \quad \mathbf{V} = \mathbf{V}_t \pm i p \Lambda_i(\omega) \tilde{\mathbf{V}}_t + p \check{\mathbf{V}}_t + p\beta \mathbf{V}_g + \mathcal{O}_{H^1}(p^2) \quad \text{as} \quad p \to 0, \tag{3.67}$$

where $\Lambda_i(\omega) = \sqrt{\frac{I(\omega)}{1+I(\omega)}} > 0$ with $I(\omega) > 0$ given by the explicit expression (3.76) below and β is uniquely defined in (3.83) below.

Simultaneously, the spectral stability problem (3.47) admits a pair of eigenvalues λ with $\mathrm{Re}(\lambda) \neq 0$ symmetric about the imaginary axis, and the eigenvector $\mathbf{V} \in H^1(\mathbb{R})$ such that

$$\lambda = \pm p \Lambda_r(\omega) + \mathcal{O}(p^3), \quad \mathbf{V} = \mathbf{V}_g \pm p \Lambda_r(\omega) \tilde{\mathbf{V}}_g + p \check{\mathbf{V}}_g + p\alpha \mathbf{V}_t + \mathcal{O}_{H^1}(p^2) \quad \text{as} \quad p \to 0, \tag{3.68}$$

where $\Lambda_r = (1-\omega^2)^{1/2} > 0$ and α is uniquely defined in (3.82) below.

We proceed with formal expansions, which are similar to the expansions (3.30). However, because the $\mathcal{O}(p)$ terms appear explicitly in the spectral stability problem (3.47), we introduce the modified expansions as follows,

$$\begin{aligned} \lambda &= p\Lambda_1 + p^2 \Lambda_2 + \mathcal{O}(p^3), \\ \mathbf{V} &= \mathbf{V}_0 + p(\Lambda_1 \mathbf{V}_1 + \check{\mathbf{V}}_1 + \mathbf{V}_0') + p^2 \mathbf{V}_2 + \mathcal{O}_{H^1}(p^3), \end{aligned} \tag{3.69}$$

where $\mathbf{V}_0$ and $\mathbf{V}_0'$ are spanned independently by the eigenvectors (3.15), $\mathbf{V}_1$ is spanned by the generalized eigenvectors (3.16), $\check{\mathbf{V}}_1$ is spanned by the vectors (3.49), and $\mathbf{V}_2$ satisfies the linear inhomogeneous equation

$$\mathcal{H}\mathbf{V}_2 = (i\Lambda_1 \mathcal{S} - \mathcal{P})(\Lambda_1 \mathbf{V}_1 + \check{\mathbf{V}}_1 + \mathbf{V}_0') + i\Lambda_2 \mathcal{S} \mathbf{V}_0. \tag{3.70}$$

By Fredholm's alternative, there exists a solution $\mathbf{V}_2 \in H^1(\mathbb{R})$ of the linear inhomogeneous equation (3.70) if and only if Λ_1 is found from the quadratic equation

$$\langle \mathbf{W}_0, (i\Lambda_1 \mathcal{S} - \mathcal{P})(\Lambda_1 \mathbf{V}_1 + \check{\mathbf{V}}_1 + \mathbf{V}_0') \rangle_{L^2} = 0, \tag{3.71}$$

where $\mathbf{W}_0$ is again spanned by the eigenvectors (3.15) independently of $\mathbf{V}_0$. Similar to (3.32), the matrix eigenvalue problem (3.71) is diagonal with respect to the translational and gauge symmetries. As a result, subsequent computations can be constructed independently for the two corresponding eigenvectors.

Selecting $\mathbf{V}_0 = \mathbf{W}_0 = \mathbf{V}_g$, $\mathbf{V}_1 = \tilde{\mathbf{V}}_g$, $\check{\mathbf{V}}_1 = \check{\mathbf{V}}_g$, and $\mathbf{V}'_0 = \alpha \mathbf{V}_t$, we use (3.17), (3.20), (3.50), (3.55), (3.57), and (3.65) in the solvability condition (3.71) and obtain the quadratic equation for Λ_1 in the explicit form

$$\Lambda_1^2 \frac{\mathrm{d}}{\mathrm{d}\omega} \int_{\mathbb{R}} |U_\omega|^2 \mathrm{d}x + \frac{1}{\omega} \int_{\mathbb{R}} |U_\omega|^2 \mathrm{d}x = 0. \tag{3.72}$$

Using the explicit expression (2.11), we obtain

$$\int_{\mathbb{R}} |U_\omega|^2 \mathrm{d}x = \frac{\sqrt{1-\omega^2}}{\omega}, \quad \frac{\mathrm{d}}{\mathrm{d}\omega} \int_{\mathbb{R}} |U_\omega|^2 \mathrm{d}x = -\frac{1}{\omega^2 \sqrt{1-\omega^2}}, \tag{3.73}$$

which yield $\Lambda_1^2 = 1 - \omega^2 = \Lambda_r(\omega)^2$. Correction terms Λ_2 and α are not determined up to this order of the asymptotic expansion.

Selecting now $\mathbf{V}_0 = \mathbf{W}_0 = \mathbf{V}_t$, $\mathbf{V}_1 = \tilde{\mathbf{V}}_t$, $\check{\mathbf{V}}_1 = \check{\mathbf{V}}_t$, and $\mathbf{V}'_0 = \beta \mathbf{V}_g$, we use (3.17), (3.19), (3.50), (3.55), (3.57), and (3.64) in the solvability condition (3.71) and obtain the quadratic equation for Λ_1 in the explicit form

$$\Lambda_1^2 \int_{\mathbb{R}} \left[\omega |U_\omega|^2 + \frac{i}{2} \left(\bar{U}_\omega U'_\omega - U_\omega \bar{U}'_\omega \right) \right] \mathrm{d}x + \frac{i}{2} \int_{\mathbb{R}} \left(\bar{U}_\omega U'_\omega - U_\omega \bar{U}'_\omega \right) \mathrm{d}x = 0. \tag{3.74}$$

Expressing

$$\frac{i}{2} \int_{\mathbb{R}} \left(\bar{U}_\omega U'_\omega - U_\omega \bar{U}'_\omega \right) \mathrm{d}x = \int_{\mathbb{R}} \frac{(1-\omega^2)^2}{(1+\omega \cosh(2\mu x))^2} \mathrm{d}x = \sqrt{1-\omega^2} I(\omega),$$

and

$$\int_{\mathbb{R}} \left[\omega |U_\omega|^2 + \frac{i}{2} \left(\bar{U}_\omega U'_\omega - U_\omega \bar{U}'_\omega \right) \right] \mathrm{d}x = \sqrt{1-\omega^2} \left[1 + I(\omega) \right], \tag{3.75}$$

where

$$I(\omega) := (1-\omega^2) \int_0^\infty \frac{\mathrm{d}z}{(1+\omega \cosh(z))^2} = 1 - \frac{1}{\sqrt{1-\omega^2}} \log\left(\frac{1-\sqrt{1-\omega^2}}{\omega} \right) > 0, \tag{3.76}$$

we obtain $\Lambda_1^2 = -\frac{I(\omega)}{1+I(\omega)} = -\Lambda_i(\omega)^2$. Again, correction terms Λ_2 and β are not determined up to this order of the asymptotic expansion.

Note again that the nonzero values in (3.73) and (3.75) verify the nonzero values in (3.19) and (3.20), and hence, the assumption $\langle \mathbf{F}_{t,g}, \sigma \tilde{\mathbf{F}}_{t,g} \rangle_{L^2} \neq 0$ in Proposition 3.2, according to Remark 4.

Justification of the formal expansion (3.69) and the proof of Lemma 3.7 is achieved by exactly the same argument as in the proof of Lemma 3.5. The proof relies on the resolvent estimate (3.35), which is valid for the massive Gross–Neveu model, because by Propositions 3.1 and 3.2, the zero eigenvalue of the operator $\mathcal{S}\mathcal{H}$ (which has algebraic multiplicity four) is isolated from the rest of the spectrum.

Persistence of eigenvalues is proved with the symmetry in Proposition 3.6. If an eigenvalue is expressed as $\lambda = p(i\Lambda_i(\omega)+\mu_p)$ with unique $\mu_p = \mathcal{O}(p)$ and $\Lambda_i(\omega) > 0$, then nonzero real part of μ_p would contradict the symmetry of eigenvalues about the imaginary axis. Therefore, $\mathrm{Re}(\mu_p) = 0$ and the eigenvalues in the expansion (3.67) remain on the imaginary axis. On the other hand, if another eigenvalue is expressed as $\lambda = p(\Lambda_r(\omega) + \mu_p)$ with unique $\mu_p = \mathcal{O}(p)$ and $\Lambda_r(\omega) > 0$, then μ_p may have in general a nonzero imaginary part, as it does not contradict the symmetry of Proposition 3.6 for a fixed $p \neq 0$. This is why the statement of Lemma 3.7 does not guarantee that the corresponding eigenvalues in the expansion (3.68) are purely real.

In the end of this section, we will show that $\mu_p = \mathcal{O}(p^2)$, which justifies the $\mathcal{O}(p^3)$ bound for the eigenvalues in the asymptotic expansions (3.67) and (3.68). In this procedure, we will uniquely determine the parameters β and α in the same asymptotic expansions. Extending the expansion (3.69) to $p^3\Lambda_3$ and $p^3\mathbf{V}_3$ terms, we obtain the linear inhomogeneous equation

$$\mathcal{H}\mathbf{V}_3 = (i\Lambda_1\mathcal{S} - \mathcal{P})\mathbf{V}_2 + i\Lambda_2\mathcal{S}(\Lambda_1\mathbf{V}_1 + \check{\mathbf{V}}_1 + \mathbf{V}_0') + i\Lambda_3\mathcal{S}\mathbf{V}_0. \tag{3.77}$$

The Fredholm solvability condition

$$\langle \mathbf{W}_0, (i\Lambda_1\mathcal{S} - \mathcal{P})\mathbf{V}_2 + i\Lambda_2\mathcal{S}(\Lambda_1\mathbf{V}_1 + \check{\mathbf{V}}_1 + \mathbf{V}_0')\rangle_{L^2} = 0 \tag{3.78}$$

determines the correction terms Λ_2, β, and α uniquely. Indeed, using (3.17) and (3.50), we rewrite the solvability condition (3.78) in the form

$$\begin{aligned} i\langle \mathbf{W}_0, \mathcal{S}\mathbf{V}_1\rangle_{L^2}\Lambda_2\Lambda_1 &= -\langle \mathbf{W}_0, (i\Lambda_1\mathcal{S} - \mathcal{P})\mathbf{V}_2\rangle_{L^2} \\ &= -\langle (-i\bar{\Lambda}_1\mathcal{S} - \mathcal{P})\mathbf{W}_0, \mathbf{V}_2\rangle_{L^2} \\ &= -\langle \mathcal{H}(-\bar{\Lambda}_1\mathbf{W}_1 + \check{\mathbf{W}}_1), \mathbf{V}_2\rangle_{L^2} \\ &= -\langle (-\bar{\Lambda}_1\mathbf{W}_1 + \check{\mathbf{W}}_1), \mathcal{H}\mathbf{V}_2\rangle_{L^2} \\ &= -\langle (-\bar{\Lambda}_1\mathbf{W}_1 + \check{\mathbf{W}}_1), i\Lambda_2\mathcal{S}\mathbf{V}_0 \\ &\quad +(i\Lambda_1\mathcal{S} - \mathcal{P})(\Lambda_1\mathbf{V}_1 + \check{\mathbf{V}}_1 + \mathbf{V}_0')\rangle_{L^2}, \end{aligned}$$

where we have used the linear inhomogeneous equation (3.70) and have introduced $\mathbf{W}_1$ and $\check{\mathbf{W}}_1$ from solutions of the inhomogeneous equations $\mathcal{H}\mathbf{W}_1 = i\mathcal{S}\mathbf{W}_0$ and $\mathcal{H}\check{\mathbf{W}}_1 = -\mathcal{P}\mathbf{W}_0$. Using

$$\langle \mathbf{W}_1, i\mathcal{S}\mathbf{V}_0\rangle_{L^2} = \langle \mathbf{W}_1, \mathcal{H}\mathbf{V}_1\rangle_{L^2} = \langle \mathcal{H}\mathbf{W}_1, \mathbf{V}_1\rangle_{L^2} = \langle i\mathcal{S}\mathbf{W}_0, \mathbf{V}_1\rangle_{L^2} = -i\langle \mathbf{W}_0, \mathcal{S}\mathbf{V}_1\rangle_{L^2}$$

and

$$\begin{aligned} \langle \check{\mathbf{W}}_1, i\mathcal{S}\mathbf{V}_0\rangle_{L^2} &= \langle \check{\mathbf{W}}_1, \mathcal{H}\mathbf{V}_1\rangle_{L^2} = \langle \mathcal{H}\check{\mathbf{W}}_1, \mathbf{V}_1\rangle_{L^2} \\ &= -\langle \mathcal{P}\mathbf{W}_0, \mathbf{V}_1\rangle_{L^2} = -\langle \mathbf{W}_0, \mathcal{P}\mathbf{V}_1\rangle_{L^2} = 0, \end{aligned}$$

where the last equality is due to (3.55), we rewrite the solvability equation in the form

$$2i\langle \mathbf{W}_0, \mathcal{S}\mathbf{V}_1\rangle_{L^2}\Lambda_2\Lambda_1 = -\langle(-\bar{\Lambda}_1\mathbf{W}_1 + \check{\mathbf{W}}_1), (i\Lambda_1\mathcal{S} - \mathcal{P})(\Lambda_1\mathbf{V}_1 + \check{\mathbf{V}}_1 + \mathbf{V}_0')\rangle_{L^2}. \tag{3.79}$$

Removing zero entries by using (3.17), (3.50), and (3.55), we rewrite Eq. (3.79) in the form

$$\begin{aligned} 2i\langle \mathbf{W}_0, \mathcal{S}\mathbf{V}_1\rangle_{L^2}\Lambda_2\Lambda_1 = \Lambda_1^2 \Big(& i\langle \mathbf{W}_1, \mathcal{S}\mathbf{V}_0'\rangle_{L^2} + i\langle \mathbf{W}_1, \mathcal{S}\check{\mathbf{V}}_1\rangle_{L^2} \\ & - i\langle \check{\mathbf{W}}_1, \mathcal{S}\mathbf{V}_1\rangle_{L^2} - \langle \mathbf{W}_1, \mathcal{P}\mathbf{V}_1\rangle_{L^2}\Big) \\ & + \langle \check{\mathbf{W}}_1, \mathcal{P}\check{\mathbf{V}}_1\rangle_{L^2} + \langle \check{\mathbf{W}}_1, \mathcal{P}\mathbf{V}_0'\rangle_{L^2}. \end{aligned} \tag{3.80}$$

We shall now write Eq. (3.80) explicitly as the 2-by-2 matrix equation by using $\mathbf{V}_0 = \mathbf{W}_0 = \Phi_V^{(0)}$, $\mathbf{V}_1 = \mathbf{W}_1 = \Phi_V^{(1)}$, $\check{\mathbf{V}}_1 = \check{\mathbf{W}}_1 = \Phi_V^{(2)}$, and

$$\mathbf{V}_0' = \Phi_V^{(0)} \begin{bmatrix} 0 & \alpha \\ \beta & 0 \end{bmatrix} = \big[\beta\mathbf{V}_g, \alpha\mathbf{V}_t\big].$$

Using (3.17), (3.51), (3.56), (3.57), and (3.58), we rewrite Eq. (3.80) in the matrix form

$$\begin{aligned} 2i\begin{bmatrix} \langle \mathbf{V}_t, \mathcal{S}\tilde{\mathbf{V}}_t\rangle_{L^2} & 0 \\ 0 & \langle \mathbf{V}_g, \mathcal{S}\tilde{\mathbf{V}}_g\rangle_{L^2} \end{bmatrix}\Lambda_2\Lambda_1 =\; & i\Lambda_1^2\begin{bmatrix} \langle \tilde{\mathbf{V}}_t, \mathcal{S}\mathbf{V}_t\rangle_{L^2} & 0 \\ 0 & \langle \tilde{\mathbf{V}}_g, \mathcal{S}\mathbf{V}_g\rangle_{L^2} \end{bmatrix}\begin{bmatrix} 0 & \alpha \\ \beta & 0 \end{bmatrix} \\ & + \begin{bmatrix} \langle \check{\mathbf{V}}_t, \mathcal{P}\mathbf{V}_t\rangle_{L^2} & 0 \\ 0 & \langle \check{\mathbf{V}}_g, \mathcal{P}\mathbf{V}_g\rangle_{L^2} \end{bmatrix}\begin{bmatrix} 0 & \alpha \\ \beta & 0 \end{bmatrix} \\ & + i\Lambda_1^2\begin{bmatrix} 0 & -\langle \check{\mathbf{V}}_t, \mathcal{S}\tilde{\mathbf{V}}_g\rangle_{L^2} \\ \langle \tilde{\mathbf{V}}_g, \mathcal{S}\check{\mathbf{V}}_t\rangle_{L^2} & 0 \end{bmatrix} \\ & - \Lambda_1^2\begin{bmatrix} 0 & \langle \tilde{\mathbf{V}}_t, \mathcal{P}\tilde{\mathbf{V}}_g\rangle_{L^2} \\ \langle \tilde{\mathbf{V}}_g, \mathcal{P}\tilde{\mathbf{V}}_t\rangle_{L^2} & 0 \end{bmatrix} \\ & + \begin{bmatrix} 0 & \langle \check{\mathbf{V}}_t, \mathcal{P}\check{\mathbf{V}}_g\rangle_{L^2} \\ \langle \check{\mathbf{V}}_g, \mathcal{P}\check{\mathbf{V}}_t\rangle_{L^2} & 0 \end{bmatrix}, \end{aligned} \tag{3.81}$$

where Λ_1 is defined uniquely from either solution of the quadratic Eqs. (3.72) and (3.74). Because the 2-by-2 matrix on the right-hand side of Eq. (3.81) is anti-diagonal, we obtain $\Lambda_2 = 0$ for every choice of Λ_1.

Now, we check that the coefficients α and β are uniquely determined from the right-hand side of the matrix Eq. (3.81). The coefficient α is determined for $\Lambda_1^2 = \Lambda_r(\omega)^2 > 0$ from the anti-diagonal entry

$$i\Lambda_1^2\langle \tilde{\mathbf{V}}_t, \mathcal{S}\mathbf{V}_t\rangle_{L^2} + \langle \check{\mathbf{V}}_t, \mathcal{P}\mathbf{V}_t\rangle_{L^2} = i\langle \tilde{\mathbf{V}}_t, \mathcal{S}\mathbf{V}_t\rangle_{L^2}\left(\Lambda_r(\omega)^2 + \Lambda_i(\omega)^2\right),$$

which is nonzero for every $\omega \in (0, 1)$. Therefore, we obtain from (3.81) the unique expression for α:

$$\alpha = \frac{\Lambda_r(\omega)^2 \left(\langle \tilde{\mathbf{V}}_t, \mathcal{P}\tilde{\mathbf{V}}_g \rangle_{L^2} + i \langle \check{\mathbf{V}}_t, \mathcal{S}\tilde{\mathbf{V}}_g \rangle_{L^2} \right) - \langle \check{\mathbf{V}}_t, \mathcal{P}\check{\mathbf{V}}_g \rangle_{L^2}}{i \langle \tilde{\mathbf{V}}_t, \mathcal{S}\mathbf{V}_t \rangle_{L^2} \left(\Lambda_r(\omega)^2 + \Lambda_i(\omega)^2 \right)}. \tag{3.82}$$

Similarly, the coefficient β is determined for $\Lambda_1^2 = -\Lambda_i(\omega)^2 < 0$ from the anti-diagonal entry

$$i\Lambda_1^2 \langle \tilde{\mathbf{V}}_g, \mathcal{S}\mathbf{V}_g \rangle_{L^2} + \langle \check{\mathbf{V}}_g, \mathcal{P}\mathbf{V}_g \rangle_{L^2} = -i \langle \tilde{\mathbf{V}}_g, \mathcal{S}\mathbf{V}_g \rangle_{L^2} \left(\Lambda_i(\omega)^2 + \Lambda_r(\omega)^2 \right),$$

which is nonzero for every $\omega \in (0, 1)$. Therefore, we obtain from (3.81) the unique expression for β:

$$\beta = \frac{\Lambda_i(\omega)^2 \left(i \langle \check{\mathbf{V}}_g, \mathcal{S}\tilde{\mathbf{V}}_t \rangle_{L^2} - \langle \tilde{\mathbf{V}}_g, \mathcal{P}\tilde{\mathbf{V}}_t \rangle_{L^2} \right) - \langle \check{\mathbf{V}}_g, \mathcal{P}\check{\mathbf{V}}_t \rangle_{L^2}}{-i \langle \tilde{\mathbf{V}}_g, \mathcal{S}\mathbf{V}_g \rangle_{L^2} \left(\Lambda_i(\omega)^2 + \Lambda_r(\omega)^2 \right)}. \tag{3.83}$$

These computations justify the $\mathcal{O}(p^3)$ terms in the expansions (3.67) and (3.68) for the eigenvalues λ.

4 Numerical Approximations

We approximate eigenvalues of the spectral stability problems (3.21) and (3.47) with the Chebyshev interpolation method. This method has been already applied to the linearized Dirac system in one dimension in Chugunova and Pelinovsky (2006). The block-diagonalized systems in (3.21) and (3.47) are discretized on the grid points

$$x_j = L \tanh^{-1}(z_j), \quad j = 0, 1, \ldots, N,$$

where $z_j = \cos\left(\frac{j\pi}{N}\right)$ is the Chebyshev node and a scaling parameter L is chosen suitably so that the grid points are concentrated in the region, where the solitary wave U_ω changes fast. Note that $x_0 = \infty$ and $x_N = -\infty$.

According to the standard Chebyshev interpolation method (Trefethen 2000), the first derivative that appears in the systems (3.21) and (3.47) is constructed from the scaled Chebyshev differentiation matrix $\widetilde{D}_N$ of the size $(N+1) \times (N+1)$, whose each element at i^{th} row and j^{th} column is given by

$$[\widetilde{D}_N]_{ij} = \frac{1}{L} \operatorname{sech}^2\left(\frac{x_i}{L}\right) [D_N]_{ij},$$

where D_N is the standard Chebyshev differentiation matrix [see page 53 of Trefethen (2000)] and the chain rule $\frac{\mathrm{d}u}{\mathrm{d}x} = \frac{\mathrm{d}z}{\mathrm{d}x}\frac{\mathrm{d}u}{\mathrm{d}z}$ has been used. Denoting I_N as an identity matrix of the size $(N+1) \times (N+1)$, we replace each term in the systems (3.21) and (3.47) as follows:

$$\partial_x \to \widetilde{D}_N, \quad 1 \to I_N, \quad U_\omega \to \text{diag}(U_\omega(x_0), U_\omega(x_1), \cdots, U_\omega(x_N)),$$

Due to the decay of the solitary wave U_ω to zero at infinity, we have $U_\omega(x_0) = U_\omega(x_N) = 0$.

The resulting discretized systems from (3.21) and (3.47) are of the size $4(N+1) \times 4(N+1)$. Boundary conditions are naturally built into this formulation, because the elements of the first and last rows of the matrix $[\widetilde{D}_N]_{ij}$ are zero. As a result, eigenvalues from the first and last rows of the linear discretized system are nothing but the end points of the continuous spectrum in Proposition 3.1, whereas the boundary values of the vector $\mathbf{V}$ at the end points x_0 and x_N are identically zero for all other eigenvalues of the linear discretized system.

Throughout all our numerical results, we pick the value of a scaling parameter L to be $L = 10$. This choice ensures that the solitary wave solutions U_ω for all values of ω used in our numerical experiments remain nonzero up to 16 decimals on all interior grid points x_j with $1 \leq j \leq N-1$.

4.1 Eigenvalue Computations for the Massive Thirring Model

Figure 2 shows eigenvalues of the spectral stability problem (3.21) for the solitary wave (2.7) of the massive Thirring model. We set $\omega = 0$ and display eigenvalues λ in the complex plane for different values of p. The subfigure at $p = 0.2$ demonstrates our analytical result in Lemma 3.5, which predicts splitting of the zero eigenvalue of algebraic multiplicity four into two pairs of real and imaginary eigenvalues. Increasing the value of p further, we observe emergence of imaginary eigenvalues from the edges of the continuous spectrum branches, as seen at $p = 0.32$. A pair of imaginary eigenvalues coalesces and bifurcates into the complex plane with nonzero real parts, as seen at $p = 0.36$, and later absorbs back into the continuous spectrum branches, as seen in the next subfigures. We can also see emergence of a pair of imaginary eigenvalues from the edges of the continuous spectrum branches at $p = 0.915$. The pair bifurcates along the real axis after coalescence at the origin, as seen at $p = 0.93$. The gap of the continuous spectrum closes up at $p = 1$. For a larger value of p, two pairs of real eigenvalues are seen to approach each other.

Figure 3 shows how the positive imaginary and real eigenvalues bifurcating from the zero eigenvalue depends on p for $\omega = 0.5, 0, -0.5$, respectively at each row. Red solid lines show asymptotic approximations established in Lemma 3.5 for $\lambda = \Lambda_r(\omega)p$ and $\lambda = i\Lambda_i(\omega)p$. Green-filled regions in Fig. 3a, c, e denote the location of the continuous spectrum. Symbols $*$ and $+$ in Fig. 3b, d, f denote purely real eigenvalues and eigenvalues with nonzero imaginary part.

Numerical results suggest the persistence of transverse instability for any period p because of purely real eigenvalues, which come close to each other and persist for a large p. We observe a stronger instability for a larger solitary wave with $\omega = -0.5$ than for a smaller solitary wave with $\omega = 0.5$. We notice that an imaginary eigenvalue does

Fig. 2 Numerical approximations for the spectral problem (3.21) associated with the solitary wave (2.7) of the massive Thirring model at $\omega = 0$

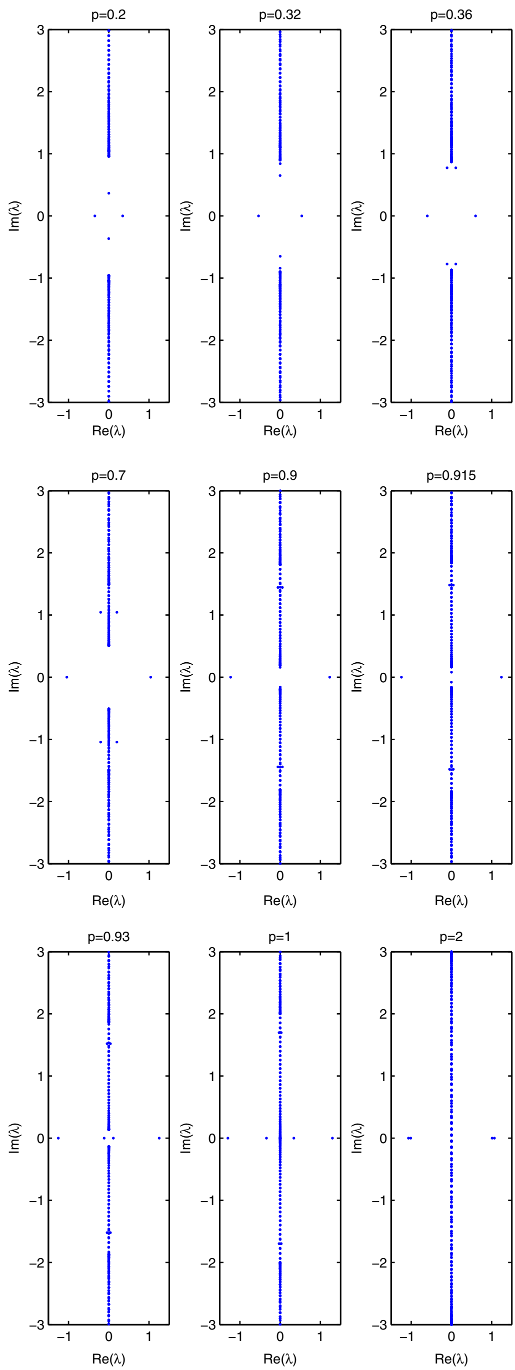

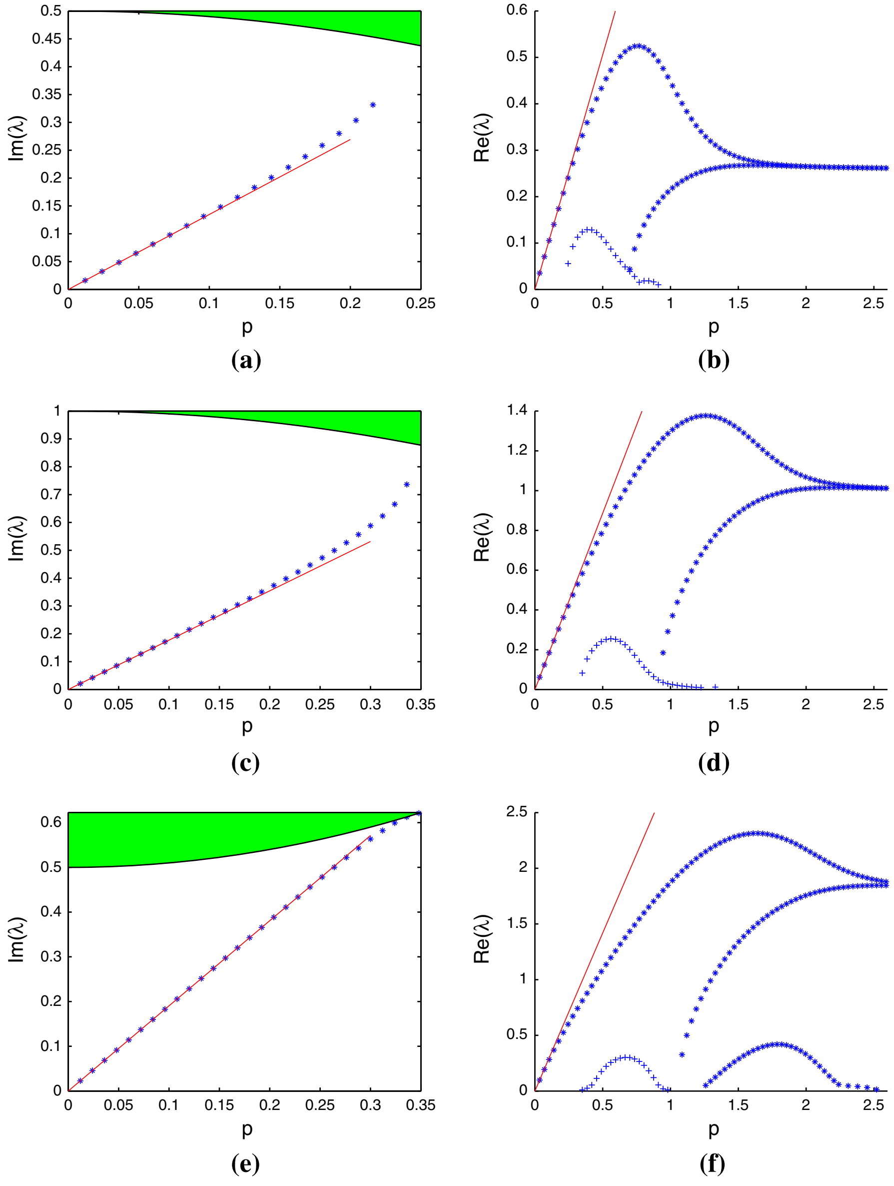

Fig. 3 Numerical approximations of isolated eigenvalues of the spectral problem (3.21) versus parameter p. **a** $\omega = 0.5$. **b** $\omega = 0.5$. **c** $\omega = 0$. **d** $\omega = 0$. **e** $\omega = -0.5$. **f** $\omega = -0.5$

not reach the edge of the continuous spectrum for $\omega = 0.5$ and $\omega = 0$ due to colliding with other imaginary eigenvalue coming from the edge of the continuous spectrum. On the other hand, an imaginary eigenvalue for $\omega = -0.5$ gets absorbed in the edge of the continuous spectrum. This is explained by the movement of the two branches of the continuous spectrum in the opposite directions: up and down as the value of p varies. Moving-down branch on $\mathrm{Im}(\lambda) > 0$, as seen in $\omega = 0.5$ and $\omega = 0$, expels

Table 1 $\max_{|\operatorname{Im}\lambda|<10}|\operatorname{Re}\lambda|$ versus values of ω and N for the spectral problem (3.21) with $p = 0$

	$\omega = -0.5$	$\omega = 0$	$\omega = 0.5$
$N = 100$	1.96×10^{-1}	2.57×10^{-1}	1.16×10^{-1}
$N = 300$	1.36×10^{-4}	2.18×10^{-4}	7.02×10^{-5}
$N = 500$	2.22×10^{-7}	8.77×10^{-5}	6.56×10^{-8}

an eigenvalue from its edge that makes collision with the other imaginary eigenvalue, while moving-up branch on $\operatorname{Im}(\lambda) > 0$, as seen in $\omega = -0.5$, absorbs an imaginary eigenvalue approaching the edge.

To verify a reasonable accuracy of the numerical method, we measure the maximum real part of eigenvalues along the imaginary axis with $|\operatorname{Im}(\lambda)| < 10$. This quantity shows the level of spurious parts of the eigenvalues, and it is known to be large in the finite difference methods applied to the linearized Dirac systems [see discussion in Chugunova and Pelinovsky (2006)]. Table 1 shows values of $\max_{|\operatorname{Im}\lambda|<10}|\operatorname{Re}\lambda|$ for three values of ω and three values of the number N of the Chebyshev points. In all numerical computations reported on Figs. 2 and 3, we choose $N = 300$; in this way, spurious eigenvalues are hardly visible on the figures.

4.2 Eigenvalue Computations for the Massive Gross–Neveu Model

Figures 4 and 5 shows eigenvalues of the spectral stability problem (3.47) for the solitary wave (2.11) of the massive Gross–Neveu equation with parameter values $\omega = 2/3$ and $\omega = 1/3$, respectively. We confirm spectral stability of the solitary wave for $p = 0$. In agreement with numerical results in Berkolaiko et al. (2015), we also observe that the spectrum of a linearized operator for $p = 0$ has an additional pair of imaginary eigenvalues in the case $\omega = 1/3$. (Recall that this issue was considered to be contradictory in the literature with some results reporting spectral instability of solitary waves for $\omega = 1/3$ in Mertens et al. 2012; Shao et al. 2014.)

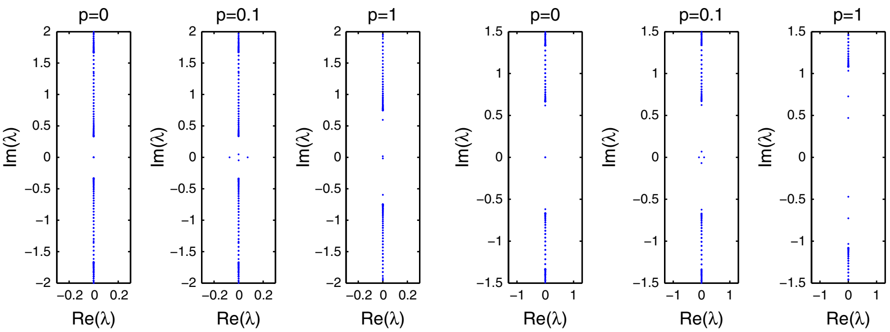

Fig. 4 Numerical approximations for the spectral problem (3.47) associated with the solitary wave (2.11) of the massive Gross–Neveu model. **a** $\omega = 2/3$. **b** $\omega = 1/3$

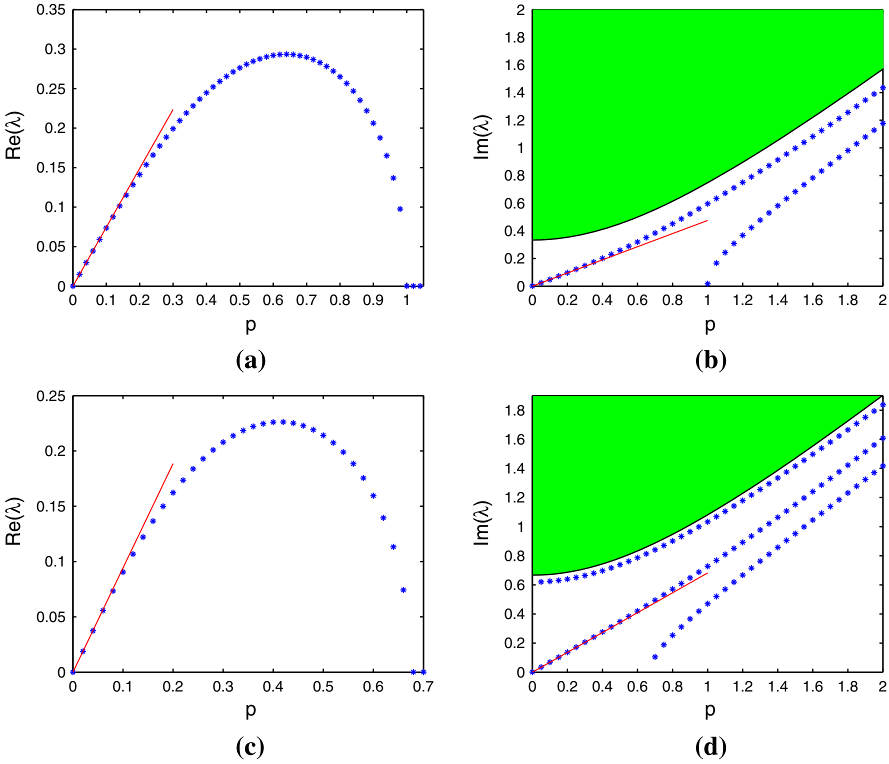

Fig. 5 Numerical approximations of isolated eigenvalues of the spectral problem (3.47) versus parameter p. **a** $\omega = 2/3$. **b** $\omega = 2/3$. **c** $\omega = 1/3$. **d** $\omega = 1/3$

The subfigures of Fig. 4 at $p = 0.1$ demonstrate our analytical result in Lemma 3.7, which predicts splitting of the zero eigenvalue of algebraic multiplicity four into two pairs of eigenvalues along the real and imaginary axes. Note that the pair along the real axis persists as the pair of real eigenvalues up to the numerical accuracy. (Recall that the statement of Lemma 3.7 lacks the result on the persistence of real eigenvalues.) Increasing the values of p further, we observe that the real eigenvalues move back to the origin and split along the imaginary axis, as seen in the subfigures at $p = 1$. The gap of the continuous spectrum branches around the origin is preserved for all values of parameter p. The pairs of imaginary eigenvalues persist in the gap of continuous spectrum for larger values of the parameter p.

Figure 5 shows real and imaginary eigenvalues versus p for the same cases $\omega = 2/3$ and $\omega = 1/3$. The green-shaded region indicates the location of the continuous spectrum. Red solid lines show asymptotic approximations established in Lemma 3.7 for $\lambda = \Lambda_r(\omega)p$ and $\lambda = i\Lambda_i(\omega)p$. It follows from our numerical results that the transverse instability has a threshold on the p values so that the solitary waves are spectrally stable for sufficiently large values of p. These thresholds on the transverse instability were observed for other values of ω in (0, 1).

Table 2 $\max_{|\operatorname{Im}\lambda|<10} |\operatorname{Re}\lambda|$ versus values of ω and N for the spectral problem (3.47) with $p = 0$

	$\omega = 1/3$	$\omega = 2/3$
$N = 100$	6.48×10^{-2}	2.03×10^{-3}
$N = 300$	1.72×10^{-2}	1.68×10^{-3}
$N = 500$	1.38×10^{-2}	1.20×10^{-3}

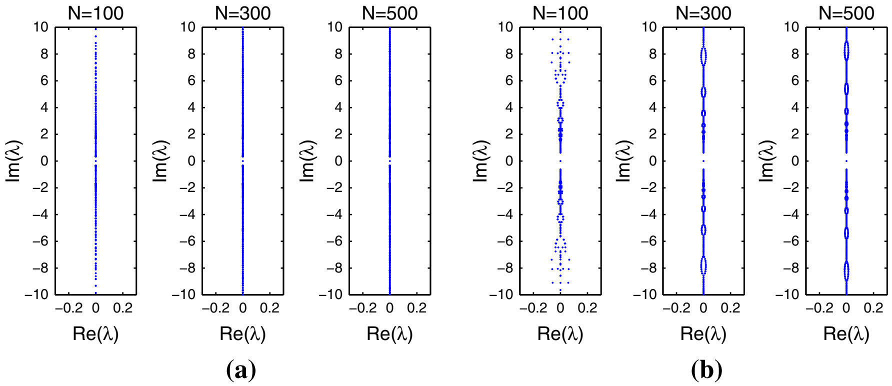

Fig. 6 Numerically computed λ for the spectral problem (3.47) with $p = 0$ for different values of the number N of Chebyshev points. **a** $\omega = 2/3$. **b** $\omega = 1/3$

To control the accuracy of the numerical method, we again compute the values of $\max_{|\operatorname{Im}\lambda|<10} |\operatorname{Re}\lambda|$ for spurious parts of eigenvalues along the imaginary axis. Table 2 shows the result for two values of ω and three values of N. Compared to Table 1, we observe a slower convergence rate and lower accuracy of our numerical approximations.

We found that spurious eigenvalues are more visible for smaller values of ω, in particular, for the value $\omega = 1/3$, evidenced in Fig. 6. While spurious eigenvalues in the case of $\omega = 1/3$ in Fig. 6 are quite visible, the maximum real part of eigenvalues with $|\operatorname{Im}\lambda| < 2$ is much smaller for $N = 400$. As a result, the value $N = 400$ was chosen for numerical approximations reported on Figs. 4 and 5, and this choice guarantees that spurious eigenvalues are hardly visible on the figures.

5 Discussion

In this last section, we discuss our main result, Theorem 3.3, in connection with the more general massive Dirac equations (2.2) and (2.9). One way to consider the more general case without going into too many technical details is to study reductions in the massive Dirac equations to the nonlinear Schrödinger (NLS) equation. Both families of solitary waves (2.7) and (2.11) have reductions to the NLS solitary wave in the limit of $\omega \to 1$. Here we explore reductions to the two-dimensional NLS equation starting with the massive Dirac equations (2.2) and (2.9). Justification of these reductions to the

NLS equation (in a more complex setting of infinitely many coupled NLS equations) can be found in the recent work (Pelinovsky et al. 2012).

5.1 Small-Amplitude Solitary Waves for the Periodic Stripe Potentials

Starting with the massive Dirac equations (2.2) for the periodic stripe potentials, we can use the scaling transformation

$$\begin{cases} u(x,y,t) = \epsilon e^{it} U(\epsilon x, \epsilon y, \epsilon^2 t), \\ v(x,y,t) = \epsilon e^{it} V(\epsilon x, \epsilon y, \epsilon^2 t), \end{cases} \tag{5.1}$$

where ϵ is a formal small parameter, and rewrite the system in the equivalent form

$$\begin{cases} V - U + i\epsilon U_X + \epsilon^2 (iU_T + U_{YY}) = \epsilon^2 (\alpha_1 |U|^2 + \alpha_2 |V|^2) U, \\ U - V - i\epsilon V_X + \epsilon^2 (iV_T + V_{YY}) = \epsilon^2 (\alpha_2 |U|^2 + \alpha_1 |V|^2) V, \end{cases} \tag{5.2}$$

where $X = \epsilon x$, $Y = \epsilon y$, and $T = \epsilon^2 t$ are rescaled variables for slowly varying spatial and temporal coordinates. Proceeding now with formal expansions,

$$\begin{cases} U = W + \frac{i}{2}\epsilon W_X + \epsilon^2 \tilde{U}, \\ V = W - \frac{i}{2}\epsilon W_X + \epsilon^2 \tilde{V}, \end{cases} \tag{5.3}$$

where W is the leading-order part and $(\tilde{U}, \tilde{V})$ are correction terms, we obtain the NLS equation on W at the leading order from the condition that the correction terms $(\tilde{U}, \tilde{V})$ are bounded:

$$iW_T - \frac{1}{2} W_{XX} + W_{YY} = (\alpha_1 + \alpha_2)|W|^2 W. \tag{5.4}$$

The NLS equation (5.4) is referred to as the hyperbolic NLS equation because of the linear diffractive terms. It admits the family of Y-independent line solitary waves if $\alpha_1 + \alpha_2 > 0$, which includes both the case of the periodic stripe potentials with $\alpha_2 = 2\alpha_1 > 0$ and the case of the massive Thirring model with $\alpha_1 = 0$ and $\alpha_2 > 0$.

From the previous literature, see, e.g., recent works (Pelinovsky et al. 2014; Pelinovsky and Yang 2014) or pioneer work (Zakharov and Rubenchik 1974), it is known that the line solitary waves are unstable in the hyperbolic NLS equation (5.4) with respect to the long transverse perturbations. The spectral instability is induced by the spatial translation eigenmode, in agreement with the result of Lemma 3.5. Moreover, the instability region extends to all values of the transverse wave number p, in agreement with our numerical results on Figs. 2 and 3. Thus, our results remain applicable to the more general family of the massive Dirac equations (2.2) with $\alpha_1 + \alpha_2 > 0$ at least for small-amplitude solitary waves.

Remark 5 The case $\alpha_1 + \alpha_2 < 0$ can also be considered with a similar reduction to the two-dimensional NLS equation, but the scaling transformation (5.1) needs to be replaced by

$$\begin{cases} u(x,y,t) = \epsilon \mathrm{e}^{-it} U(\epsilon x, \epsilon y, \epsilon^2 t), \\ v(x,y,t) = \epsilon \mathrm{e}^{-it} V(\epsilon x, \epsilon y, \epsilon^2 t). \end{cases} \tag{5.5}$$

This is because the small-amplitude solitary waves bifurcate from the point $\omega = -1$ if $\alpha_1 + \alpha_2 < 0$, whereas they bifurcate from the point $\omega = +1$ if $\alpha_1 + \alpha_2 > 0$. The case $\alpha_1 + \alpha_2 = 0$ is exceptional, when the reduction to the two-dimensional NLS equation fails.

Substituting (5.5) into (2.2) and performing computations similar to (5.2) and (5.3), we obtain the elliptic NLS equation

$$iW_T + \frac{1}{2} W_{XX} + W_{YY} = (\alpha_1 + \alpha_2)|W|^2 W. \tag{5.6}$$

The Y-independent solitary waves exist if $\alpha_1 + \alpha_2 < 0$ and they are unstable with respect to long Y-periodic perturbations (Kivshar and Pelinovsky 2000; Pelinovsky and Yang 2014; Zakharov and Rubenchik 1974).

5.2 Small-Amplitude Solitary Waves for the Hexagonal Potentials

Turning now to the massive Dirac equations (2.9) for the hexagonal potentials, we can use the same scaling transformation (5.1) and obtain

$$\begin{cases} V - U + \epsilon(iU_X + V_Y) + i\epsilon^2 U_T = \epsilon^2 \left(\beta_1 (U|U|^2 + \overline{U} V^2 + 2U|V|^2) + \beta_2 \overline{U}(U^2 - V^2)\right), \\ U - V - \epsilon(iV_X + U_Y) + i\epsilon^2 V_T = \epsilon^2 \left(\beta_1 (V|V|^2 + \overline{V} U^2 + 2V|U|^2) + \beta_2 \overline{V}(V^2 - U^2)\right). \end{cases} \tag{5.7}$$

Proceeding now with formal expansions,

$$\begin{cases} U = W + \frac{\epsilon}{2}(iW_X + W_Y) + \epsilon^2 \tilde{U}, \\ V = W - \frac{\epsilon}{2}(iW_X + W_Y) + \epsilon^2 \tilde{V}, \end{cases}$$

we obtain the following NLS equation for W from the condition that the correction terms $(\tilde{U}, \tilde{V})$ are bounded:

$$iW_T - \frac{1}{2} W_{XX} - \frac{1}{2} W_{YY} = 4\beta_1 |W|^2 W. \tag{5.8}$$

The NLS equation (5.8) is referred to as the elliptic NLS equation because of the linear diffractive terms. It admits the family of Y-independent line solitary waves if $\beta_1 > 0$, which includes both the case of the hexagonal potentials with $\beta_1, \beta_2 > 0$ and the case of the massive Gross–Neveu model with $\beta_1 = -\beta_2 > 0$.

Similarly to Remark 5, if $\beta_1 < 0$, one can use the scaling transformation (5.5) and derive the elliptic NLS equation

$$iW_T + \frac{1}{2}W_{XX} + \frac{1}{2}W_{YY} = 4\beta_1 |W|^2 W. \tag{5.9}$$

However, the case $\beta_1 = 0$ is exceptional, when the reduction to the elliptic NLS equation fails.

It is well known from the previous literature, see, e.g., Kivshar and Pelinovsky (2000), Pelinovsky and Yang (2014), Zakharov and Rubenchik (1974), that the line solitary waves are unstable in the elliptic NLS equations (5.8) and (5.9) with respect to the long transverse perturbations. The spectral instability is induced by the gauge rotation eigenmode, in agreement with the result of Lemma 3.7. Moreover, the instability band has a finite threshold on the transverse wave number p, in agreement with our numerical results in Figs. 4 and 5. Thus, our results remain applicable to the more general family of the massive Dirac equations (2.9) with $\beta_1 \neq 0$ and arbitrary β_2 at least for small-amplitude solitary waves.

5.3 Summary

To summarize, we proved analytically for the massive Thirring and Gross–Neveu models in two spatial dimensions that the line solitary waves are unstable with respect to the transverse perturbations of sufficiently long periods. We approximated eigenvalues of the transverse stability problem numerically and showed that the instability region extends to the transverse perturbations of any period for the massive Thirring model, but it has a finite threshold for the massive Gross–Neveu model. Based on the small-amplitude reduction to the hyperbolic or elliptic NLS equations, we extended this conclusion to the more general massive Dirac equations in two spatial dimensions which model periodic stripe and hexagonal potentials in the two-dimensional Gross–Pitaevskii equation.

Acknowledgments The authors thank A. Comech and P. Kevrekidis for useful discussions of the numerical part of this work. D.P. is supported by the NSERC grant. Y.S. is supported by a graduate scholarship of the Department of Mathematics at McMaster University.

References

Ablowitz, M.J., Zhu, Y.: Nonlinear waves in shallow honeycomb lattices. SIAM J. Appl. Math. **72**, 240–260 (2012)

Ablowitz, M.J., Zhu, Y.: Nonlinear wave packets in deformed honeycomb lattices. SIAM J. Appl. Math. **73**, 1959–1979 (2013)

Berkolaiko, G., Comech, A., Sukhtayev, A.: Vakhitov–Kolokolov and energy vanishing conditions for linear instability of solitary waves in models of classical self-interacting spinor fields. Nonlinearity **28**, 577–592 (2015)

Berkolaiko, G., Comech, A.: On spectral stability of solitary waves of nonlinear Dirac equations in 1D. Math. Model. Nat. Phenom. **7**(2), 13–31 (2012)

Boussaid, N., Comech, A.: On spectral stability of the nonlinear Dirac equation. arXiv:1211.3336 (2012)

Candy, T.: Global existence for an L^2-critical nonlinear Dirac equation in one dimension. Adv. Differ. Eqs. **7–8**, 643–666 (2011)

Chugunova, M., Pelinovsky, D.: Block-diagonalization of the symmetric first-order coupled mode system. SIAM J. Appl. Dyn. Syst. **5**, 55–83 (2006)

Contreras, A., Pelinovsky, D.E., Shimabukuro, Y.: L^2 orbital stability of Dirac solitons in the massive Thirring model. arXiv:1312.1019 (2013)

Dohnal, T., Aceves, A.B.: Optical soliton bullets in (2+1)D nonlinear Bragg resonant periodic geometries. Stud. Appl. Math. **115**, 209–232 (2005)

Fefferman, C.L., Weinstein, M.I.: Honeycomb lattice potentials and Dirac points. J. Am. Math. Soc. **25**, 1169–1220 (2012a)

Fefferman, C.L., Weinstein, M.I.: Waves in honeycomb structures, Journees Equations aux derivees partialles, Biarretz, 3–7 juin 2012, GDR 243 4 (CNRS) (2012b)

Fefferman, C.L., Weinstein, M.I.: Wave packets in honeycomb structures and two-dimensional Dirac equations. Commun. Math. Phys. **326**, 251–286 (2014)

Gross, D.J., Neveu, A.: Dynamical symmetry breaking in asymptotically free field theories. Phys. Rev. D **10**, 3235–3253 (1974)

Huh, H.: Global solutions to Gross–Neveu equation. Lett. Math. Phys. **103**, 927–931 (2013)

Hoq, Q.E., Gagnon, J., Kevrekidis, P.G., Malomed, B.A., Franzeskakis, D.J., Carretero-Gonzáles, R.: Extended nonlinear waves in multidimensional dynamical lattices. Math. Comput. Simul. **80**, 721–731 (2009)

Johnson, M.A.: The transverse instability of periodic waves in Zakharov–Kuznetsov type equations. Stud. Appl. Math. **124**, 323–345 (2010)

Johnson, M.A., Zumbrun, K.: Transverse instability of periodic traveling waves in the generalized Kadomtsev–Petviashvili equation. SIAM J. Math. Anal. **42**, 2681–2702 (2010)

Kevrekidis, P.G., Gagnon, J., Franzeskakis, D.J., Malomed, B.A.: X, Y, and Z waves: extended structures in nonlinear lattices. Phys. Rev. E **75**, 016607 (2007)

Kivshar, YuS, Pelinovsky, D.E.: Self-focusing and transverse instabilities of solitary waves. Phys. Rep. **331**, 117–195 (2000)

Mertens, F.G., Quintero, N.R., Cooper, F., Khare, A., Saxena, A.: Nonlinear Dirac equation solitary waves in external fields. Phys. Rev. E **86**, 046602 (2012)

Pelinovsky, D.E.: Localization in Periodic Potentials: From Schrödinger Operators to the Gross–Pitaevskii Equation. London Mathematical Society lecture note series 390. Cambridge University Press, Cambridge (2011)

Pelinovsky, D.: Survey on global existence in the nonlinear Dirac equations in one dimension. In: Ozawa, T., Sugimoto, M. (eds.) Harmonic Analysis and Nonlinear Partial Differential Equations, vol. 26. RIMS Kokyuroku Bessatsu, pp. 37–50 (2011)

Pelinovsky, D., Rousset, F., Tzvetkov, N.: Normal form for transverse instability of line solitons of the Zakharov–Kuznetsov equation, (2015, in preparation)

Pelinovsky, D.E., Ruvinskaya, E.A., Kurkina, O.A., Deconinck, B.: Short-wave transverse instabilities of line solitons of the 2-D hyperbolic nonlinear Schrödinger equation. Theor. Math. Phys. **179**, 452–461 (2014)

Pelinovsky, D., Schneider, G.: Bounds on the tight-binding approximation for the Gross–Pitaevskii equation with a periodic potential. J. Differ. Eqs. **248**, 837–849 (2010)

Pelinovsky, D.E., Shimabukuro, Y.: Orbital stability of Dirac solitons. Lett. Math. Phys. **104**, 21–41 (2014)

Pelinovsky, D.E., Simpson, G., Weinstein, M.I.: Polychromatic solitons in a periodic and nonlinear Maxwell system. SIAM J. Appl. Dyn. Syst. **11**, 478–506 (2012)

Pelinovsky, D.E., Yang, J.: On transverse stability of discrete line solitons. Phys. D **255**, 1–11 (2014)

Rousset, F., Tzvetkov, N.: Stability and instability of the KDV solitary wave under the KP-I flow. Commun. Math. Phys. **313**, 155–173 (2012)

Schneider, G., Uecker, H.: Nonlinear coupled mode dynamics in hyperbolic and parabolic periodically structured spatially extended systems. Asymptot. Anal. **28**, 163–180 (2001)

Selberg, S., Tesfahun, A.: Low regularity well-posedness for some nonlinear Dirac equations in one space dimension. Differ. Integral Eqs. **23**, 265–278 (2010)

Shao, S., Quintero, N.R., Mertens, F.G., Cooper, F., Khare, A., Saxena, A.: Stability of solitary waves in the nonlinear Dirac equations with arbitrary nonlinearity. Phys. Rev. E **90**, 032915 (2014)

Thirring, W.: A soluble relativistic field theory. Ann. Phys. **3**, 91–112 (1958)

Trefethen, L.N.: Spectral Methods in MATLAB. SIAM, Philadelphia (2000)

Yamazaki, Y.: Stability of line standing waves near the bifurcation point for nonlinear Schrödinger equations. Kodai Math. J. **38**, 65–96 (2015)

Yang, J.: Transversely stable soliton trains in photonic lattice. Phys. Rev. A **84**, 033840 (2011)

Yang, J., Gallardo, D., Miller, A., Chen, Z.: Elimination of transverse instability in stripe solitons by one-dimensional lattices. Opt. Lett. **37**, 1571–1573 (2012)
Zakharov, V.E., Rubenchik, A.M.: Instability of waveguides and solitons in nonlinear media. Sov. Phys. JETP **38**(1974), 494–500 (1974)
Zhang, Y., Zhao, Q.: Global solution to nonlinear Dirac equation for Gross–Neveu model in 1+1 dimensions. Nonlinear Anal. Theory Methods Appl. **118**, 82–96 (2015)